Annu. Rev. Astron. Astrophys. 1992. 30: 185–233

THE PLUTO-CHARON SYSTEM

S. A. Stern[1]

Center for Astrophysics and Space Astronomy, University of Colorado, Boulder, Colorado 80309

KEY WORDS: planets, solar system

1. OVERVIEW

Over sixty years after its discovery, Pluto remains an astronomer's planet: Unlike the other planets it has not been visited by a spacecraft, and therefore remains studied only through astronomical and astrophysical techniques.

This review summarizes the present-day state of knowledge about Pluto and Charon, pointing out inconsistencies and critical obstacles to further progress. It is largely restricted to what I call the "modern era" of Pluto studies, beginning in 1976. Therefore, Section 2 only briefly describes the chronology of progress from the time of Pluto's discovery through the mid-1970s; Section 3 briefly summarizes the present state of knowledge about Pluto's orbit and its orbit history; Section 4 reviews our current understanding of the Pluto-Charon system's bulk parameters; Sections 5, 6, and 7 then describe what is known about Pluto's surface, interior, and atmosphere, respectively; Section 8 summarizes the state of knowledge about Charon's physical properties; Section 9 discusses theories of the origin of the Pluto-Charon system; finally, Section 10 gives some perspective on where we have come and where we are going in the study of this unique, binary-planet system.

2. HISTORICAL CONTEXT

The study of Pluto may be categorized as having undergone four historical phases: search and discovery (up to 1930), early work (1931–1950), classical observations (1950–1975), and the modern era (1976–present). It can be

[1] Now at Southwest Research Institute, Division 15/Space Sciences, 6220 Culebra Road, San Antonio, Texas 78238.

0066–4146/92/0915–0185$02.00

said that we are now just entering a fifth phase, the era of space observations, which should enjoy major advances from the *Hubble Space Telescope* (*HST*), the *Far Ultraviolet Spectroscopic Explorer* (*FUSE*), the *Space Infrared Telescope Facility* (*SIRTF*), and other satellites over the next 20 years. With hard work and luck, a sixth era, comprising a spacecraft mission to Pluto, should reach culmination in the mid-2010s or early 2020s.

This section briefly reviews what was discovered and known prior to 1975, in order to provide historical context for what follows. For a more detailed account of the period prior to 1930, the reader is referred to Whyte's (1980) unmatched, 140-page account of the search for Pluto, its discovery, and the first five decades of its study.

Pluto was discovered in February, 1930 by C. W. Tombaugh after a long search for the strong perturber of Uranus and Neptune that we now know never existed (cf Tombaugh & Moore 1980, Hoyt 1980). Unfortunately, the originator of that search, Percival Lowell, did not live to see Pluto's discovery. After the determination of its orbit, no important discoveries were made about Pluto until the early 1950s.

Between 1953 and 1976, however, technological advances made possible several important findings. Among these were the determination through photoelectric photometry of Pluto's $\sim$6.39 day rotation period (Walker & Hardie 1955), the detection of Pluto's intrinsically red color (Fix et al 1970), and the discovery of Pluto's high axial obliquity (Andersson & Fix 1973) and its 3:2 orbital resonance with Neptune (Cohen & Hubbard 1965, Williams & Benson 1971).

Beginning in 1976, the pace of discoveries increased even more dramatically. In rapid succession, came the discovery of methane on Pluto's surface (Cruikshank et al 1976); the detection of Pluto's satellite Charon (Christy & Harrington 1978, 1980); the prediction (Andersson 1978), detection (Binzel et al 1985), and then study of the once-every-124 year mutual eclipse event season (cf Binzel 1989 for a good review); the occultation of Pluto by a bright star in 1988, confirming the presence of an atmosphere (e.g. Elliot et al 1989); and the 1989 *Voyager 2* Neptune-system encounter, which gave us important, detailed insights into Pluto's closest-analog in the Solar System: Triton. It is largely the findings and progress of this modern era of Pluto exploration that are reviewed here.

3. PLUTO'S ORBIT, ROTATION, AND POLE POSITION

3.1 *Heliocentric Orbit*

Six decades of observation have now yielded accurate orbital elements for Pluto; relative to the other known planets, Pluto's orbit is unusually

eccentric ($e \approx 0.25$), inclined ($i \approx 17$ deg), and large ($a \approx 39.6$ AU). Pluto's orbit period is 248 years, during which the planet ranges from inside Neptune (perihelion near 29.7 AU) to near the edge of the putative Kuiper Disk (aphelion near 49.5 AU), causing the surface insolation to vary by factors of 3. The Pluto-Charon barycenter passed perihelion at 05.1 ± 0.1 September 1989 UT.

Seidelmann et al (1980) have given a history of the study of Pluto's orbital elements. They report that as of 1980, orbit integrations using osculating elements give Pluto's position to no better than 1–2 arc-sec accuracy over timescales of a decade. However, improvement is now expected from the more accurate gravitational mass (GM) values for the giant planet systems derived from *Pioneer 11* and *Voyager* spacecraft flybys of the 1980s.

Pluto's perihelion lies inside Neptune's orbit (Neptune's semimajor axis is 30.1 AU and its orbit is less than 1% eccentric). It was recognized in mid-1930, the year of Pluto's discovery, that this unprecedented situation would lead to close approaches which would limit the dynamical lifetime of Pluto's orbit to 10^6–10^7 yrs unless something prevented them. Something does. In the mid-1960s, it was shown that Pluto's orbit exhibits a 3:2 resonance with Neptune which prevents mutual close approaches through a longitude libration. The Pluto-Neptune separation is maintained because the argument of Pluto's perihelion (i.e. the angle between the perihelion position and the position of its ascending node) librates around 90 degrees with an amplitude of ± 23 deg. This ensures that Pluto is never near perihelion when in conjunction with Neptune. That is, Pluto is "protected" because Neptune passes Pluto's longitude only near Pluto's aphelion, never allowing Neptune approaches closer than ≈ 17 AU. Indeed, Pluto approaches Uranus more closely than Neptune, with a minimum separation of ≈ 11 AU (too far to significantly perturb Pluto's orbit). The discovery of Pluto's libration about the exact 3:2 Neptune commensurability (Cohen & Hubbard 1965) has been verified by a series of increasingly longer simulations of the outer Solar System (Williams & Benson 1971, Nacozy & Deihl 1974, Appelgate et al 1986), now exceeding 8×10^8 years (Sussman & Wisdom 1988).

Pluto's orbit also exhibits a second libration with a period close to 3.78×10^7 years. Pluto is thus known to undergo at least two confirmed resonances, one in mean motion, the other a secular resonance. Additionally, Appelgate et al (1986) and then Sussman & Wisdom (1988) have found other resonances with periods including 1.37×10^8, and 6×10^8 years. Sussman & Wisdom's calculations also revealed a Lyapunov coefficient, γ, of $10^{-7.3}$ yr^{-1}, which corresponds to a Lyapunov timescale of 2×10^7 years. A positive Lyapunov coefficient indicates a degree of

sensitivity to initial conditions which they classify as chaotic. Milani et al (1989) reexamined the chaos issue. They claim that the positive gamma Sussman & Wisdom found is probably a numerical artifact induced by model sensitivity to their adopted value of Neptune's mass. Milani et al report that, rather than a positive Lyapunov coefficient, Pluto in fact exhibits a 246 Myr 3:1 "super resonance" between the circulation and libration of two secular arguments, which merely manifests itself as $\gamma > 0$ in the Sussman & Wisdom results. Milani et al then suggest that although Pluto may be formally chaotic on some unknown timescale, its complex resonance structure may actually engender long-term orbit stability. The study of Pluto's orbital dynamics and stability remains open at present, and one looks forward to additional results as computational capabilities allow investigators to increasingly improve the fidelity and timebase of their simulations.

3.2 *Rotation Period and Pole*

As indicated above, Pluto's photometric lightcurve varies regularly (Walker & Hardie 1955) with a period of 6.387 days (Hardie 1965, Andersson & Fix 1973, Neff et al 1974, Binzel & Mulholland 1983). Hardie's (1965) report was also the first to note the secular increase in Pluto's lightcurve amplitude, which has now persisted since at least 1955. Although the 6.387 day period is identical to Charon's orbit period (see Section 4), Charon's photometric contribution is too small to account for the lightcurve's full amplitude, implying that the lightcurve period is indeed Pluto's rotation period. Pluto's lightcurve period has remained in phase (i.e. not precessed) for decades. Figure 1 shows the shape of the combined Pluto-Charon lightcurve, and its evolution over the past few decades.

Andersson & Fix (1973) were the first to report Pluto's polar obliquity. Using the variation of the lightcurve amplitude from the 1950s to the early 1970s and the change in Pluto's spin vector orientation as seen from Earth, they determined an obliquity of 90 ± 40 degrees. Dobrovolskis & Harris (1983) made a more recent determination of 118.5 deg, which has now been superseded by the results of the Pluto-Charon mutual events. Based on the mutual-event (mutual eclipse) solutions given by Tholen & Buie (1989, 1990), Pluto's obliquity can be calculated to be 122 ± 1 deg; the corresponding pole position is near declination -9 deg, right ascension 312 deg (equator and equinox of 1950). As first noted by Dobrovolskis & Harris (1983), torques in the Pluto-Charon binary cause Pluto's obliquity to oscillate with an $\sim 3 \times 10^6$ year period. Based on the post–mutual event obliquity estimate, the obliquity should range between ~ 105 and ~ 130 deg over time. Those concerned with long-term dynamics and seasonal cycles should also note that although Pluto presently reaches perihelion

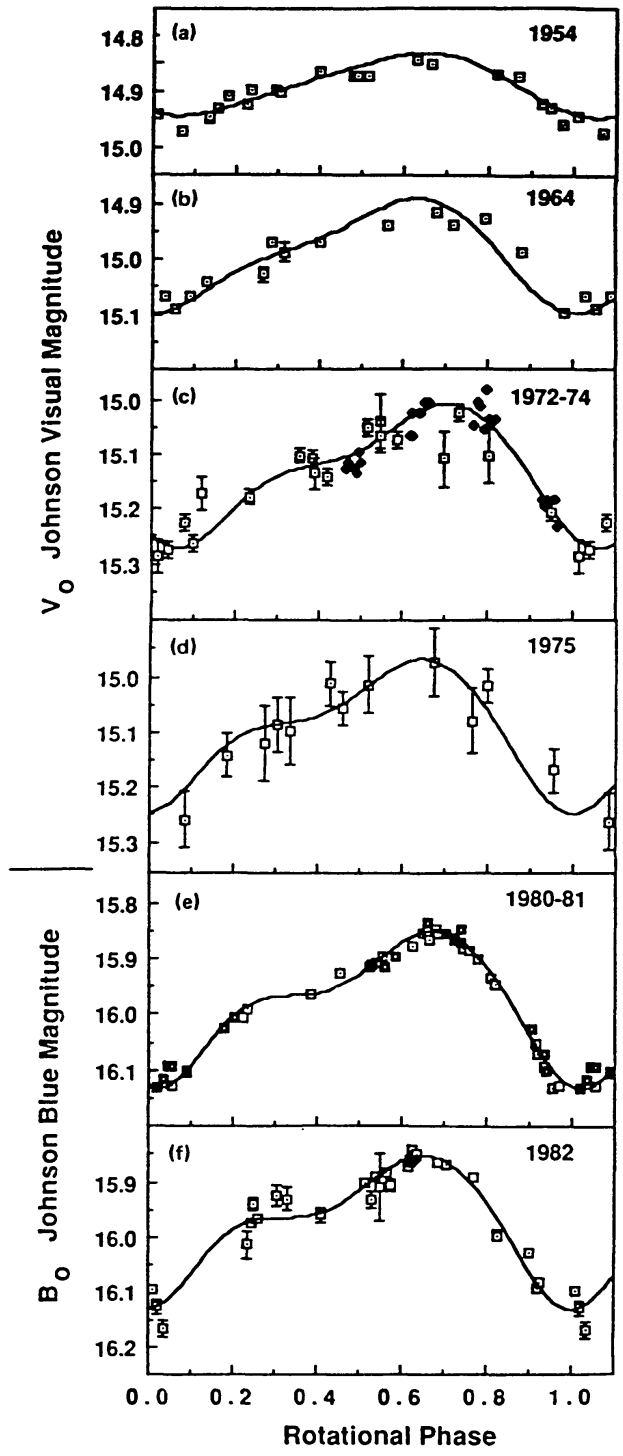

Figure 1 The evolution of Pluto's lightcurve; adapted from Marcialis (1988).

with its pole vector nearly normal to the Sun, and roughly coincident with the orbit velocity vector, this configuration is coincidental, since the pole executes a circulation with a 3.7×10^6 year precession period with respect to Pluto's orbit normal.

4. CHARON'S DISCOVERY, THE MUTUAL EVENTS, AND THE BASIC ATTRIBUTES OF THE PLUTO-CHARON SYSTEM

4.1 *Discovery*

Our knowledge of the basic, or bulk parameters of the Pluto-Charon system fundamentally derive from the discovery of Charon. Before that, for example, Pluto's radius was uncertain to factors of four and Pluto's mass was uncertain to a factor of almost 100. Dessler & Russell (1978) parodied this situation in an article titled, "The Impending Disappearance of Pluto."

Charon (typically pronounced variously like Kharon and Sharon) was discovered on a series of photographic plates made in 1978 at the US Naval Observatory Flagstaff Station. These plates were taken less than four miles from Lowell Observatory, where Pluto was discovered 48 years before. Charon was apparent as a regular cycle of elongations on the Pluto images. It is not surprising that Charon was so difficult to detect, since it never appears more than 1 arc-sec from Pluto as seen from Earth, and its V magnitude never much exceeds 16. J. W. Christy and R. S. Harrington described Charon's discovery and orbit in a series of four papers (Christy & Harrington 1978, 1980; Harrington & Christy 1980, 1981) in which they determined that Charon's orbit is (*a*) synchronous with Pluto's rotation and (*b*) highly inclined to the plane of the ecliptic. Historical accounts of this discovery have been given by Marcialis (1988) and Whyte (1980). Burns (1986) and Peale (1986) discussed the dynamical evolution of the Pluto-Charon binary and its stable synchronous configuration in some detail.

Given Charon's discovery in 1978 and *Voyager*'s discoveries of many small satellites in the 1980s, it would seem natural to ask whether Pluto too may have additional satellites. Although Charon orbits 2×10^4 km from Pluto, Pluto's tidal stability domain stretches some 4×10^6 km in diameter. Stern et al (1991b) undertook a CCD search for other satellites, but found none. They were able to show that at $>90\%$ confidence, no other satellites brighter than 22nd magnitude exist outside Charon's orbit. This magnitude constraint corresponds to bodies with Charon-like geometric albedos ($A = 0.4$) as small as 37 km in radius.

4.2 *Charon's Orbit and the System Mass*

The evidence that Charon orbits Pluto with a period equal to Pluto's long-established rotation period immediately implies the system had reached complete spin-orbit synchronicity: an unprecedented situation in all the Solar System. Although there is no data to the contrary, the strict demonstration of *complete* tidal evolution awaits the demonstration that Charon is not rotating with a period different from its orbit. Synchronicity is widely expected because standard tidal theory shows that Charon's internal rotation will synchronize to its orbit period (as is the case for many planetary satellites), 10–100 times faster than Pluto's rotation period becomes locked to the satellite's orbit period (cf also Farinella et al 1979), which we know has already occurred.

Table 1 gives a baseline set of Charon orbital elements adopted from Tholen & Buie's (1990) mutual event solutions to the orbit; many dozen mutual events observed between 1985 and 1989 went into this fit. To establish an absolute scale, Tholen & Buie adopted the recent semimajor axis determination of $a = 19{,}640 \pm 320$ km derived by Beletic et al (1989) from speckle-interferometric data obtained in 1984 and 1985. This value of the semimajor axis is now widely quoted. It is statistically indistinguishable from the direct-imaging CCD result obtained by Jones et al (1988) of $a = 19{,}558 \pm 153$ km, and supercedes previous determinations (e.g. Harrington & Christy 1980, Bonneau & Foy 1980, Hegè & Drummond 1984,

Table 1 Orbital and physical parameters for Pluto and Charon

Semimajor axis	**19,640**	**± 320**	**km**
Eccentricity	**0.0002**	**± 0.0021**	
Inclination[a]	**98.9**	**± 1.0**	**deg**
Ascending node[a]	**222.407**	**± 0.024**	**deg**
Argument of periapsis[a]	**210**	**± 31**	**deg**
Mean anomaly[b]	**259.96**	**± 0.08**	**deg**
Epoch	**JDE 2,446,600.5**	**= 1986 June 19**	
Period	**6.387246**	**± 0.000011**	**days**
Pluto radius	**1151**	**± 6**	**km**
Charon radius	**593**	**± 13**	**km**
Pluto blue geometric albedo	**0.61**	**(0.44 - 0.61)**	
Charon blue geometric albedo	**0.378**	**± 0.015**	
Mean density	**2.029**	**± 0.032**	**g cm^{-3}**

[a] Referred to the mean equator and equinox of 1950.0.
[b] Measured from the ascending node.
From Tholen & Buie (1990).

Tholen 1985) which gave similar, but less precise results. Further improvements in the semimajor axis are expected to result from future stellar occultations and *HST* observations of Pluto and Charon against background stars begun in 1991.

Several important insights are to be gained from our present knowledge of Charon's orbit. First among these is that, based on Charon's known orbital period and the Beletic et al (1989) semimajor axis, one derives a system (i.e. combined Pluto+Charon) mass of $1.35 \pm 0.07 \times 10^{-8}\ M_{\odot}$ or $1.47 \pm 0.08 \times 10^{25}$ g. This is very small, just $2.5 \times 10^{-3}\ M_{\text{earth}}$. Second, dynamical studies by Weissman et al (1989) have shown that tides efficiently damp both the planet/satellite relative rotational angular momentum vectors and the angle between Charon's equator and Charon's orbital pole on a timescale of $< 10^6$ years. This implies that Charon should orbit over Pluto's equator and be spin-aligned with Pluto. Observations show this is at least approximately true, but sufficient resolution is not available to detect any small, potentially interesting, deviations from this equilibrium state. Third, the mutual event solutions show that unless Charon's line of apsides lies essentially on the line of sight to Earth, then Charon's orbital eccentricity is very low, formally $\approx 10^{-4}$ (though uncertainties in the solution probably still permit $e \approx 10^{-3}$). This very circular orbit is a natural result of the orbital synchronicity described above.

Around Pluto-Charon's perihelion, Charon's orbital plane appears to be nearly coincident with the North-South direction on the sky. Shortly after Charon's discovery, Andersson (1978) pointed out that Pluto's orbital motion would cause Charon's orbital plane to sweep through the line of sight to the Earth for a period of several years every half-Pluto-orbit, or 124 terrestrial years. Mutual eclipses would then occur every 3.2 days (half Charon's orbit period) during each mutual event epoch. Over a period of 5–6 years, these eclipses were predicted to progress from brief, shallow, partial events, through central events lasting up to five hours (from 1st to 4th contact), and then recede again to shallow events. Figure 2 illustrates the mutual event geometry.

4.3 *The Pluto-Charon Mutual Events*

Andersson's important realization opened up the possibility of studying the Pluto-Charon system with the powerful techniques developed for eclipses between stellar binaries. The initial prediction by Andersson indicated that the events could have (fortuitously in a 124-year window) started as early as 1979. As Charon's orbit pole position was refined, however, the predicted onset date moved to 1983–1986. (This too was fortuitous, since knowledge of the pole could have changed to indicate that the events had

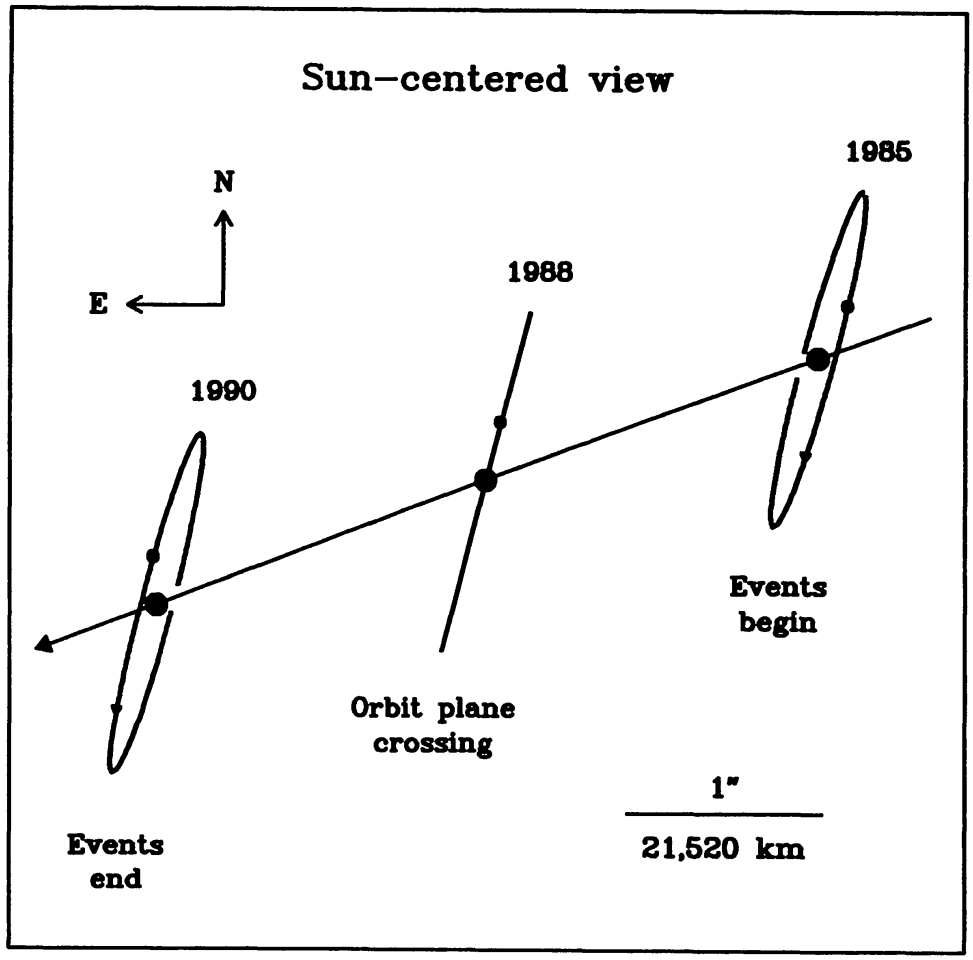

Figure 2 The Pluto-Charon mutual event geometry; provided with permission by R. L. Marcialis.

already taken place in the 1970s!) After a multi-year effort by several groups to detect the onset of such events, the first definitive eclipse detections were made on February 17, 1985 by R. P. Binzel at McDonald Observatory, and confirmed 3.2 days later on February 20, 1985 by D. J. Tholen at Mauna Kea. These first, shallow events ($\sim$0.01–0.02 mag) of Pluto and Charon moving across one another's poles were reported by Binzel et al (1985).

The very existence of these eclipses proved the claim (by 1985 widely accepted) that Charon was in fact a satellite, rather than some incredible topographic feature. The eclipse season persisted until October 1990, and over 100 event observations have been reported by various observers. Important results from the Pluto-Charon mutual events include surface maps of Pluto and Charon, individual albedos and spectra, and improvements in Charon's orbit. Of greatest relevance, however, was the

opportunity to use event timing to accurately determine the radii of Pluto and Charon.

4.4 *The Radii and Average Density of Pluto and Charon*

Prior to the mutual events, the radii of Pluto and Charon were highly uncertain. A well-observed near-miss occultation of Pluto in 1965 (Halliday et al 1966) had constrained Pluto's diameter to <6800 km, but no better. Circumstantial evidence for Pluto's small size (compared to the terrestrial planets) was inferred from (*a*) the combination of Pluto's $m_V \approx 14$ magnitude and the discovery of CH_4 frost on Pluto (see Section 5) which exhibits an intrinsically high albedo, and (*b*) the low system mass determined after the discovery of Charon. However, since Pluto and Charon remained unresolved in terrestrial telescopes (their apparent diameters are <0.1 arc-sec), direct measurements of their diameters were not accurate.

Attempts to remedy the situation came in several forms. First, Walker (1980) reported the results of a stellar occultation by Charon on April 7, 1980. The 50-second length of Walker's positive detection, observed using a 1-m telescope at Sutherland South Africa, gave an absolute lower limit for Charon's radius of 600 km. The Charon result is in agreement with Walker's (1980) occultation lower limit, and Elliot & Young's (1991a) reanalysis of Walker's data, giving an improved radius lower limit of 601.5 ± 0.8 km (3σ). Clearly, Walker was fortunate to observe a practically central occultation. A set of radii constraints obtained using speckle techniques were reported in the early 1980s (e.g. Hegè et al 1982), but these are now known to have been in error by factors as great as two.

Yet another set of radii measurements result from fits of the mutual event lightcurves. From a careful analysis of such data, Tholen & Buie (1990) find radii solutions of 1151 ± 6 and 593 ± 13 km for Pluto and Charon, respectively. However, Elliot et al (1989) find that the stellar occultation of Pluto observed in 1988 (see Section 7.2) indicates the presence of a haze layer which may have biased the mutual occultation results toward a higher Pluto radius. According to Elliot and coworkers, Pluto's radius could be as small as 1000–1050 km—up to 100–150 km smaller than the mutual event radius if the haze interpretation is correct. Elliot & Young (1991b) showed that if the thermal-gradient interpretation for their occultation lightcurve is correct (cf Section 7.2), Pluto's radius could be as large as 1210 km. The resolution of this important discrepancy awaits (*a*) better knowledge of Charon's semimajor axis (on which the mutual event radii depend), (*b*) better knowledge of limb darkening effects at Pluto and Charon, and (*c*) observations of additional stellar occultations.

Still, it is clear that the sizes of both Pluto and Charon are probably now known to better than 10%, and perhaps to 3%. The two striking

implications of these results are (*a*) that Pluto and Charon form the best example of a double planet in the Solar System, and (*b*) that Pluto is a very small planet—smaller than any other known, and indeed, smaller than at least seven planetary satellites (Luna, Io, Europa, Ganymede, Callisto, Titan, and Triton).

Based on the now-established volumes of Pluto and Charon, and the total mass of the binary, it is possible to derive a system-average density of 2.03 ± 0.2 g cm^{-3}. The error in this estimate is based on the Tholen & Buie (1990) radii solution, with allowance made for the potential semi-major axis scale uncertainties described above. If Elliot et al's ≈ 1000 km lower-limit radius for Pluto is correct, the system density could climb to 2.6 g cm^{-3}. Densities of 1.8–2 g cm^{-3} or higher imply that the system is internally dominated by rocky material. This result and its implications will be discussed in more detail in Section 6, where models for Pluto's density and internal structure are described.

5. PLUTO'S SURFACE PROPERTIES

5.1 *Recent Progress*

Pluto's surface properties have been studied since the 1970s by photometric, spectroscopic, and polarimetric techniques. The bandpass available for study has expanded from the classical, ground-based window in the 1970s to include the reflected IR and the vacuum ultraviolet. Thermal IR measurements of the Pluto-Charon binary have also been made (discussed in Section 7).

Here we proceed as follows. First, photometric measurements of Pluto's albedo, solar phase function, color, and polarimetric properties will be discussed. This will be followed by a discussion of spectroscopic data relating to Pluto's surface composition. Finally, we will discuss Pluto's probable disk-resolved surface appearance, based on lightcurve and mutual event data; this discussion will include a brief review of work on surface topography and cratering. Related data for Charon are presented in Section 8.

5.2 *Albedo and Color*

Accurate knowledge of Pluto's albedo was only obtained after the onset of the mutual events, because until then Pluto's radius was unknown, and further, there was no definitive way of removing Charon's contribution. However, prior to the eclipses, the presence of surface CH_4 (Cruikshank et al 1976, Lebofsky et al 1979) gave circumstantial evidence that Pluto's albedo was likely to be high. The very first report of eclipse detections (Binzel et al 1985) gave more information, revealing ~ 2 times different

depths for partial eclipses of Charon and Pluto, indicating Pluto's polar geometric albedo is substantially higher than Charon's. Subsequently, various groups, including Tholen et al (1987), Dunbar & Tedesco (1987), and Reinsch & Pakull (1988), made initial estimates of Pluto's global albedo from the expanding eclipse data set.

Now that the eclipse season is complete, a more complete data set is available for analysis. Comprehensive models for the analysis of mutual event lightcurve data (cf Dunbar & Tedesco 1987, Tholen & Buie 1988) must simultaneously solve for the individual radii, the individual albedos, and Charon's orbital elements. The solution for these parameters is made more complicated by varying solar phase angle effects, the presence of shadows during eclipse events, and instrumental and timing uncertainties. To derive the albedo lightcurve for Pluto alone, one first derives Pluto's albedo at the longitude of the total, superior eclipses (in which Charon's signal was completely removed), and then scales the rest of the lightcurve albedo from this point, assuming Charon's rotational lightcurve has negligible effect on the combined Pluto+Charon lightcurve. The superior events occur at 0.75 rotational phase, corresponding to Plutocentric longitudes centered around 0 degrees. The assumption that a constant Charon contribution can be removed is made because (*a*) its geometric cross-section is small compared to Pluto's, (*b*) its eclipsed hemisphere has a geometric albedo about 50–60% of Pluto's, and (*c*) its visible-wavelength slope of the wavelength-dependent albedo is virtually zero (i.e. colorless). (However, cf Section 8; some data now indicate Charon's visible lightcurve may be non-negligible.)

Tholen & Buie (1990) have analyzed a large set of mutual event data in this way to find Pluto's maximum, disk-integrated blue geometric albedo to be 0.61, with rotational variations taking the blue, disk-integrated albedo as low as 0.44. Somewhat better results will be available upon completion of eclipse data analysis, which in principle will both (*a*) reduce errors in the fits and (*b*) allow time-resolved differential measurements of each body to be inverted to yield surface maps (see below for initial results). However, the most important gains will come with the derivation of complete, multi-color independent lightcurves.

Information on Pluto's color comes from both unresolved photometry of the binary and the mutual events. As reported in Section 2, Pluto's visible-bandpass color slope has been known to be red for almost two decades. The most recent analysis of pre–mutual event photometry yields $B-V$ and $U-B$ color differences of 0.842 and 0.31 respectively for Pluto+Charon combined (Tholen 1985). Buie & Tholen (1989) also report weak evidence that Pluto has reddened since the 1950s. The potential causes of such reddening are discussed below. Binzel (1988) analyzed eclipse data

to derive the color of Pluto's anti-Charon hemisphere and found that $B-V = 0.867 \pm 0.008$ mag. All of these results confirm that Pluto's surface color is mildly red. By comparison, Pluto's $B-V$ color is much less red than the refractory surfaces of Mars ($B-V = 1.36$) and Io ($B-V = 1.17$), and slightly redder than its hydrocarbon-rich analog, Triton ($B-V = 0.72$).

Barker et al (1980) reported the first modern study of Pluto's near-UV spectrum. Presenting evidence showing Pluto's reddish color-slope extends throughout the 3500–7350 Å bandpass, Barker et al pointed out that this is distinctly different from the majority of Saturnian and Uranian satellites, which are essentially colorless, but similar to the water-ice covered Galilean satellites of Jupiter ($0.83 < B-V < 0.87$), though this color similarity may not result from the same mechanism.

Stern et al (1991a) used the *International Ultraviolet Explorer* (*IUE*) spacecraft to measure the albedo and lightcurve properties of the combined system in the 2600–3200 Å UV range at six rotational phases between $\theta = 0.46$ and $\theta = 0.70$ (i.e. around lightcurve maximum). Pluto + Charon's UV geometric albedo was found to be $p_{uv} = 0.25 \pm 0.05$, about half the Johnson blue albedos in this same region. This is a result of Pluto's color slope, which causes the albedo to decline toward the blue. By contrast, Triton's UV albedo is much higher, $p_{uv} = 0.55 \pm 0.05$, which may indicate Triton's frosts are less radiation damaged (and therefore perhaps younger) than Pluto's. This implies that Pluto's UV albedo is *anti*correlated with B and 1–2.5 μ IR magnitude albedo at the rotational phases explored by *IUE*. This anticorrelation implies that the $B-UV$ color difference reaches a maximum around Pluto + Charon's maximum light, which may be attributable to either a weakly UV-absorbing surface contaminant on Pluto at these longitudes or a very strongly UV-absorbing agent on Charon's surface.

5.3 *Phase Curve and Polarimetry*

The photometric behavior of the changes in brightness of a planet or satellite as it approaches opposition can be used to derive surface scattering properties. Knowledge of the complete solar phase curve is also required to transform geometric albedos into bolometric Bond albedos. For Pluto + Charon combined Andersson & Fix (1973) found a linear solar phase coefficient of 0.05 mag/deg in the visible; Marcialis (1983) found 0.031 ± 0.01 mag/deg; Binzel & Mulholland (1984) reported 0.041 ± 0.003 mag/deg. D. J. Tholen (unpublished) found 0.037 ± 0.002 mag/deg. Because the Pluto-Charon system has only been observed from the vicinity of the Earth, no measurements of the large-angle scattering behavior have been made. Pluto's maximum solar phase angle (ϕ_{max}) around the time of

perihelion, as seen from the 1 AU baseline provided by the Earth at quadrature, is just ≈ 1.9 deg. Therefore, no certain derivation of the phase integral q or planetary Bond albedo A can be made. Some increase in knowledge should become possible if *Galileo* observes Pluto from its orbit about Jupiter, where $\phi_{max} \approx 10$ deg, or if the *Cassini* orbiter obtains Pluto's phase curve to $\phi_{max} \approx 18$ deg from orbit about Saturn; however, what is really needed are flyby spacecraft measurements of Pluto at high-phase angles. For the present, the best available phase integral to use for Pluto is probably Triton's (Pluto and Triton have similar linear phase coefficients; Triton's is 0.027 mag/deg; Goguen et al 1989). Triton's q has been measured by *Voyager* (Smith et al 1989), giving $q = 1.2$ (green) to 1.5 (violet). If Pluto is similar, then surface units may have Bond albedos ranging from 0.3 to 0.5.

We now turn to polarimetric measurements of the Pluto-Charon binary. The first polarimetric measurements of this system were made by Kelsey & Fix (1973), who obtained a plane polarization coefficient of $0.27 \pm 0.02\%$, in the scattering plane (this is called "negative polarization"), using a broad visible-wavelength bandpass. Breger & Cochran (1982) reported further measurements made from 1979 to 1981 giving a similar plane polarization coefficient of $0.29 \pm 0.01\%$. No convincing evidence of rotational modulation in the polarization was seen in either the Kelsey & Fix or Breger & Cochran data sets. This is somewhat surprising since Pluto's lightcurve shows almost 30% amplitude. It is also surprising that Pluto's polarization did not change in a statistically significant way, either between 1972 and 1981 (during which Pluto's lightcurve amplitude and overall brightness changed considerably, cf Figure 1), or as a function of solar phase angle (in contrast to most asteroid surfaces). Breger & Cochran speculate that Pluto's unusual polarization behavior could be explained by counteracting surface and atmospheric effects. An alternative explanation is that Pluto's bright frost-covered surface simply does not show the strong solar phase angle dependent polarization that asteroidal regoliths do.

5.4 *Surface Composition*

The first identification of a spectrally active surface constituent on Pluto was the discovery by Cruikshank et al (1976) of evidence for CH_4 absorption bands at 1.7 and 2.3 μ. Cruikshank et al noted that these absorptions could represent methane frost itself, or a methane–water ice clathrate ($CH_4 \times H_2O$). In this same report, evidence was also presented for the lack of strong H_2O and NH_3 absorptions in the IR. Based on the identification of CH_4, Cruikshank and coworkers were able to presciently conclude that Pluto is bright, and therefore small and of low mass. Direct confirmation

of the methane detection came when Benner et al (1978) detected additional, but weaker CH_4 absorption bands between 0.7 and 0.9 μ, and again when Lebofsky et al (1979) made new IR photometric measurements resolving the structure of the 1.7 μ and 2.3 μ CH_4 bands. Lebofsky et al reported that Pluto's IR spectrum was better matched by CH_4 frost than CH_4 hydrate laboratory methane frosts. Spectroscopic studies by Fink et al (1980), Soifer et al (1980), and Apt et al (1983) allowed more realistic fits to laboratory data. The discovery of weak CH_4 bands on Triton (Cruikshank & Silvaggio 1979) and H_2O-ice bands on the Uranian satellites further intensified interest in Pluto (cf. Cruikshank & Brown 1986 for an excellent summary of Triton and Uranian satellite work).

Rotationally resolved spectra of Pluto's CH_4 red and infrared bands have been variously reported by Buie & Fink (1987), Sawyer et al (1987), Spencer et al (1990), and Marcialis & Lebofsky (1991). Buie and Fink (Buie 1984, Buie & Fink 1987) studied the red bands of CH_4. Their data demonstrated that although Pluto's methane is present at all rotational epochs, the band depths are correlated with the lightcurve such that the least absorption occurs at minimum light. Mutual event spectroscopy has now demonstrated that Charon could not be the cause of this variation, since its surface is devoid of detectable CH_4 absorptions (see Section 8). This important discovery implies that Pluto's dark regions could be reaction products resulting from the photochemical (Stern et al 1988) or radiological (Johnson 1989) conversion of methane to more complex hydrocarbons or graphite. Marcialis & Lebofsky (1991) produced a high-quality data set confirming Buie and Fink's findings, and extended the albedo/CH_4 correlation to the IR bands between 1 and 2.3 μ. In recent work, Spencer et al (1990) have used 3–4 μ spectrophotometry to study both the CH_4 ν_3 fundamental (the deepest of CH_4's absorption features) and search for the equivalents of laboratory features due to H_2O, CO, CO_2, and NH_3. Spencer et al found a good match to the CH_4, but no evidence of any other constituents.

It is important to note that all published information on Pluto's methane coverage is restricted to longitudinal (rather than latitudinal) studies. We are thus left today with the following picture of Pluto's surface composition: CH_4 appears rotationally ubiquitous, with surface coverage coupled to albedo. Pluto's strong lightcurve and red color demonstrate that at least one other widespread, probably involatile surface constituent exists. This may be either rocky material, or more naturally, hydrocarbons resulting from radiation processing of the CH_4. Whether the frost we are seeing is a surface veneer or the major component of Pluto's crust is unclear.

For the future, one looks forward to more sensitive searches for other surface frosts, and latitudinally-resolved compositional data sets, both of which are important to atmospheric and volatile transport models.

5.5 *Surface Appearance and Markings*

Progress in describing Pluto's surface appearance has come on two fronts: studies of lightcurve evolution and mutual event photometry. While the lightcurve work is now well advanced, most of the mutual event photometry remains unreduced for the purpose of surface mapping.

Evidence for surface markings on Pluto has been available since the mid-1950s, when Walker & Hardie (1955) first detected rotational modulation of the lightcurve. Because Pluto is large enough to be essentially spherical (and indeed, mutual event and stellar occultation data show it actually is), the distinct signatures of this lightcurve can be correlated with widescale-albedo features. Examining Figure 1 again, it is clear that Pluto's surface must contain at least three major provinces: a dark region near 0 phase, a somewhat brighter region around 0.25 phase, and a very bright region around lightcurve maximum near 0.75 phase. Additional information can be gained by observing the evolution of this lightcurve as Pluto moves around its orbit while the pole position remains inertially fixed—assuming, of course, that the surface albedo distribution is time invariant.

Stern et al (1988) have questioned the time-invariant assumption owing to Pluto's highly volatile, and thus mobile, surface frost. However, we restrict our attention here to the fixed-spot models, and the tests of their accuracy. This fixed vs variable albedo pattern controversy will be discussed further in Section 7 as a part of the description of Pluto's atmospheric and seasonal cycles.

The first serious attempt to model Pluto's surface appearance was the lightcurve analysis of Lacis & Fix (1972). Using a Fourier decomposition (an inverse technique) these workers were able to show Pluto's bright and dark units have substantially different albedos. However, as shown by Russell (1906), such a technique is unable to decompose a lightcurve into a *unique* albedo distribution. Following this, Marcialis (1983, 1988) constructed a simple but functional two-spot plus latitudinal band solution that reproduces the main attributes of Pluto's lightcurve and lightcurve evolution from the 1950s to the early 1980s. The difference between Marcialis' technique and that of Lacis & Fix is that Marcialis used a forward- (rather than inverse-) solving, finite elements approach with several simplifying assumptions (e.g. equatorially-centered spots darker than the surrounding terrain in the ratio 2 : 1) to reduce the size of the solution space.

Buie & Tholen (1989) produced a second model for the appearance of Pluto's surface. Their more complete model includes data made primarily in B (with some V data) from 1954–1986, as well as selected mutual event data from 1988. Like Marcialis' model, Buie & Tholen assumed a

time-invariant surface, circular spots, and an unspotted Charon. However, this model also included an improved representation of the sub-earth latitude history on Pluto, and made use of Hapke's bidirectional reflectance theory for surface albedo. After a careful search of parameter space, a "best-fit" solution was obtained. This solution, called the SHELF model in Buie & Tholen's terminology, has two nearly-equatorial spots and two nearly-polar spots (or caps). Like the Marcialis model, near-equatorial spots reproduce the rotational lightcurve, while polar caps and a broad equatorial albedo band reproduce the orbital lightcurve variation. The primary differences between this solution and Marcialis' are: (*a*) one light and one dark equatorial spot is preferred here, rather than two dark spots, (*b*) differing spot sizes, albedos, and contrast to the background surface albedo, and (*c*) an off-center (latitude 81 deg, rather than an exactly polar) spot in the northern hemisphere. A Buie & Tholen model solution is depicted in Figure 3. Notice the dark equatorial band. Notice also that the two remaining latitudinal "bands" in this "best" solution are actually polar caps, with the largest being on Pluto's northern hemisphere.

Both the Marcialis and Buie & Tholen Pluto maps are nonunique (each model involves about two dozen free parameters). Still, it is likely these maps represent the gross albedo pattern of Pluto with some fidelity. The greatest value of these models is that they provide reference solutions against which mutual-event-derived maps, *HST*-imaging, and a priori theoretical volatile transport models can be gauged.

Before leaving the subject of Pluto's surface appearance, it is worthwhile to briefly summarize the status of color variations across its surface. On the basis of color difference measurements during mutual events Binzel (1988) found that the polar caps are relatively bluer than the surrounding "equatorial" terrain. This result may imply that Rayleigh scattering in the ice plays a role. Correspondingly, Marcialis & Lebofsky (1991) find evidence from a combination of lightcurve data and IR spectrophotometry that the dark regions on Pluto are redder than the equatorial bright spots. Thus, the dark regions may simply be areas where the long-chain hydrocarbon-photolysis byproducts of CH_4 chemistry play a more dominant role in the surface albedo and color. This result is in agreement with the earlier-mentioned result that methane is less abundant at longitudes exhibiting lower albedo. Whether this is due to volatile transport, topography, or some other combination of factors is unclear.

5.6 *Surface Topography and Crater Density*

It is fashionable to claim Pluto should look like Triton—mountains, valleys, ridges, complex "parquet-like" landforms, and some craters. How-

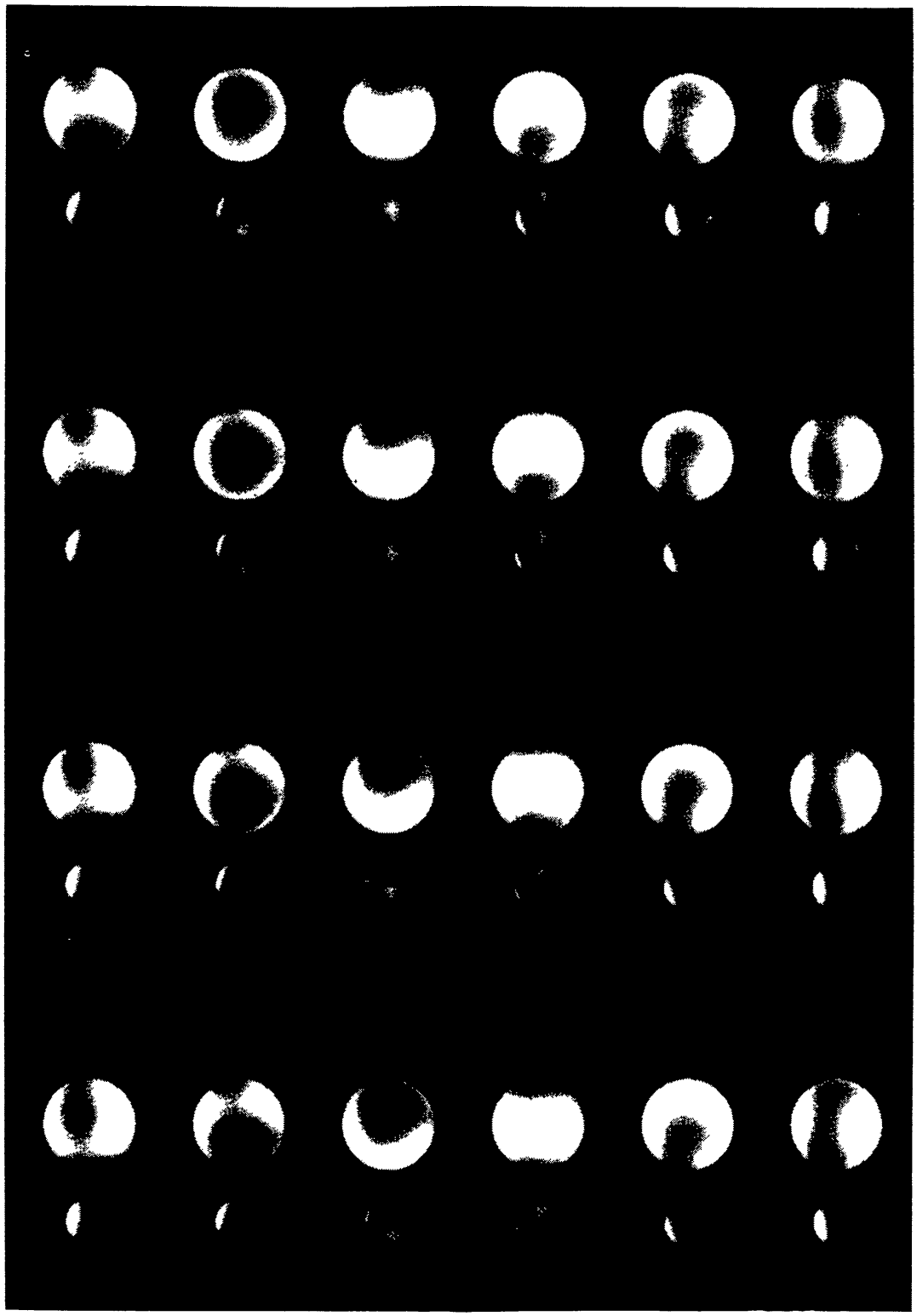

Figure 3 A collage of images showing the entire surfaces of Pluto and Charon according to mapping results derived from mutual event data, computed by M. Buie, K. Horne, and D. Tholen using a maximum entropy technique (cf also Buie & Tholen 1989). A 360 deg rotation is shown in 15 deg increments, beginning at upper left and proceeding row by row, with the north poles of Pluto and Charon at the top.

ever, the likelihood that Pluto and Triton have undergone differing thermal and bombardment histories (owing to their different dynamical niches) makes this "standard" assumption a dubious reed to rest on. Until much higher resolution data is available, however, Pluto's topographic appearance will remain a virtual unknown.

Still, despite the lack of observational constraints, three theoretical studies are worth reporting. First is work (R. L. Marcialis, personal communications 1985, 1989) indicating that the structural weakness of CH_4-ice at Pluto's surface temperature ($T \approx 50$ K) will cause steep-sloped or large-scale topographic (>10 km) features to mechanically relax on geologic timescales. This implies that any such topography on Pluto is likely to be supported by rheologically stronger materials, such as water ice or rock. If steep-sloped features are eventually found to be common, one might conclude that the ubiquitous CH_4 provides only a veneer over a more abundant and stronger crustal or mantle material.

In a second study, Weissman et al (1989) used the flux of short and long-period comets to estimate the cometary cratering rate on Pluto. They find that Kuiper Disk comets likely dominate the present-day flux, with expected cratering rates in the range 10^{-13}–10^{-12} craters km^{-2} yr^{-1} (for both long and short-period comets). Typical impact speeds are estimated to be 4–5 km s^{-1}. Over 5×10^9 years, Pluto is expected to have accumulated $\sim 10^3$ cometary impact craters typically 70–150 km in diameter; this is insufficient to result in cratering saturation.

Finally, Stern (1989) pointed out that if Pluto has lost a significant amount of CH_4 to hydrodynamic escape (cf Section 7.3) then one to several km of volatile topography may have been lost to "escape erosion." For this reason, ancient terrain may not be preserved on Pluto unless it is constructed of involatile materials not subject to sublimation and escape.

6. PLUTO'S DENSITY, BULK COMPOSITION, AND INTERIOR STRUCTURE

6.1 *Density*

Post–mutual event knowledge of Charon's semimajor axis and the radii of Pluto and Charon allow us to specify the average Pluto+Charon (or system) density to 10% or better. The major remaining uncertainty in the system density is Pluto's radius, which stellar occultation measurements indicates could be 100–150 km different from the mutual event solution (see Section 7.3).

If Charon were small compared to Pluto, so that its volume comprised only a negligible fraction of the total, system volume, then Pluto's density

would be virtually the same as the system density. Unfortunately (or fortunately, depending on one's perspective), this is not the case. In fact, Charon represents between 10% and 18% of the system volume, depending on the true radii of the two bodies. This ratio is larger than any other planet-satellite pair in the Solar System. Thus, to derive Pluto's density we require an additional constraint to make the system of equations deterministic.

The most natural source of such information would be precise astrometry to determine the magnitude of the barycentric wobble, which would in turn give the mass ratio of Pluto to Charon.

In the absence of such a measurement, Stern (1988) parameterized Pluto's density in terms of Charon's density, and then allowed Charon's density to range over the wide domain from 0.9 to 5.5 g cm^{-3}. Since Charon is not *too* large, it cannot weight the system density too far. It was thus found that $1.1 < \rho_{pl} < 2.4$ g cm^{-3}, with a preferred range of $1.3 < \rho_{pl} < 2.1$ g cm^{-3}. Taking the post-eclipse radii determinations of Tholen & Buie (1990) and the system mass implied by Beletic et al's (1989) semimajor axis measurement, Stern's (1988) model today yields $1.4 < \rho_{pl} < 2.2$ g cm^{-3} for the unrestrictive range of Charon densities $0.9 < \rho_{ch} < 5.5$ g cm^{-3}. Adopting McKinnon's (1989a) dynamically-derived upper limit on Charon's density of $\rho_{ch} < 2.3$ g cm^{-3} (cf Section 8), one derives $1.8 < \rho_{pl} < 2.2$ g cm^{-3}, which is the best available formal constraint on Pluto's density one can expect until the barycentric wobble is measured.

6.2 *The Bulk Composition and Internal Structure*

The discovery that the system density, and thus Pluto's density is near 2 g cm^{-3}, was a major surprise resulting from the mutual events. Previously, Pluto's density had been expected to be ~ 1 g cm^{-3} or lower (e.g. Lupo & Lewis 1980a,b). Thus, contrary to earlier thinking, Pluto's interior dominated by material denser than water ice.

Two comprehensive analyses of Pluto's interior structure have been reported (McKinnon & Mueller 1988, Simonelli et al 1989); Stern (1988) constructed a much simpler model. In these models, Pluto's bulk density was based on the mutual event system density, and Pluto was assumed to consist of water ice ($\rho = 1.00$ g cm^{-3}), "rock" ($2.8 < \rho < 3.5$ g cm^{-3}, depending upon its degree of hydration), and perhaps methane ice ($\rho = 0.53$ g cm^{-3}). More complicated models employing multiple rock components or other volatiles (e.g. CO- or N_2-ice) are possible but are unlikely to provide additional insight, since they introduce more unknowns

than they do constraints. Using Pluto's bulk density as the only important constraint, Stern found Pluto's rock fraction almost certainly exceeds 50%, and could approach 90%. McKinnon & Mueller (1988) and Simonelli et al (1989) employed additional, cosmochemical constraints on the composition; they found rock fractions in the range 0.6–0.75, with preferred values close to 0.7. Similar models show that the large (e.g. $R > 500$ km), icy satellites of Jupiter, Saturn, and Uranus have typical rock fractions in the range 0.5–0.6 by mass. Only Triton, with $\rho = 2.05$ g cm^{-3} (Smith et al 1989, Tyler et al 1989) rivals Pluto and Charon in terms of the expected rock content. The implications of this result will be discussed in Section 9, as a part of the discussion of Pluto's origin. However, it is worth pointing out here that Pluto's present-day density may be higher than its primordial density if (for example) a Charon-forming giant impact occurred after differentiation or rapid hydrodynamic escape of a volatile atmosphere.

We now turn to the issue of Pluto's possible internal differentiation. Several lines of evidence suggest at least partial differentiation. These include (*a*) estimates of the heat generated by radiogenic decay of Pluto's large rock component, which indicate widespread melting may well have occurred (McKinnon & Mueller 1988, Simonelli et al 1989); (*b*) the possibility that accretional heating may have been sufficient to trigger differentiation (Simonelli & Reynolds 1989); (*c*) the presence of the very light material CH_4 on the surface and the fact that atmospheric escape would remove surface methane if it was intimately mixed with involatile materials (e.g. water ice), which could not themselves escape (Stern 1989); and (*d*) the possibility that the giant-impact which may be responsible for the formation of the Pluto-Charon binary could itself have been energetic enough to trigger differentiation (McKinnon 1989b). It is thus reasonable to say that several independent pathways for Pluto to differentiate appear viable, and that it is not unlikely that such differentiation actually occurred. Of course, definitive tests for Pluto's differentiation elude us today, since they require measurement of the planet's moment of inertia, its precise figure, or complete crustal composition; such measurements require a spacecraft encounter.

The gross internal thermal structure of Pluto depends on several factors, virtually all of which are unknown. These include material viscosities in the interior, the internal convection state, the actual rock fraction and radioisotope content, and the internal density distribution (i.e. most fundamentally, the differentiation state). It seems likely (Simonelli & Reynolds 1989) that Pluto's deep interior reaches temperatures of at least 100–200 K; 3–4 times higher values are not implausible (McKinnon & Mueller 1988). Whether or not Pluto is warm enough to exhibit solid-state ice

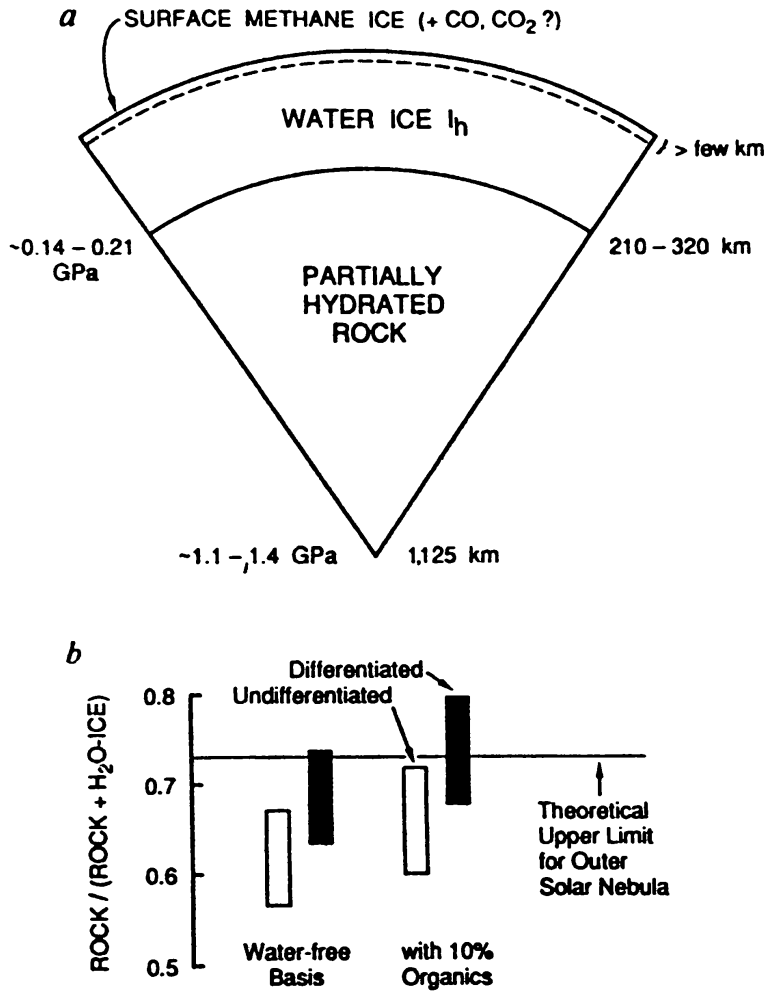

Figure 4 (*a*) A model cross-section showing Pluto's interior structure, assuming differentiation; (*b*) the dependence of Pluto's rock fraction on various circumstances. Adapted from McKinnon & Mueller (1988).

convection depends on both the internal thermal structure and the radial location of water ice in the interior; however, McKinnon & Mueller (1988) and Simonelli et al (1989) found that solid-state convection should be occurring in the water-ice layer.

Pluto's central pressure can be estimated to lie between 0.6 and 0.9 Gpa if the planet is undifferentiated, and 1.1–1.4 Gpa if differentiation has occurred (McKinnon & Mueller 1988). As such, the high-pressure water-ice phase ice VI is expected in the deep interior if the planet has not differentiated. If differentiation has occurred, ice II, may be present, but only near the base of the convection layer. If Pluto did differentiate, then its gross internal structure can be represented by a model like that shown in Figure 4.

7. PLUTO'S ATMOSPHERE

7.1 *Early Evidence*

In some workers' view, the issue of an atmosphere surrounding Pluto was settled many years prior to the benchmark, 1988 stellar occultation. This is because at the expected temperature regime on Pluto (40–55 K), methane ice will sublime and therefore develop a vapor pressure which would result in an atmosphere. Laboratory data (e.g. Brown & Ziegler 1980) made it possible to predict the CH_4 atmospheric column from first principles, given Pluto's surface temperature and gravity. However, while this is strictly correct, methane's vapor pressure curve is so steep that, without knowing the precise surface temperature, the total atmospheric methane column could be uncertain by over three orders of magnitude, from <0.1 to near 100 m-am (where 1 meter-amagat is the number abundance of a gas column 1 cm^2 in cross section and 1 meter high at standard temperature and pressure).

Another argument was advanced by Stern et al (1988). The train of logic is as follows: Radiation processes should cause surface methane to polymerize (i.e. on a timescale of a few tens of orbits), leaving behind a ubiquitous, dark (perhaps red) coating of hydrocarbons. However, Pluto's albedo is known to be very high. Thus, something has to be either hiding or replenishing the surface. We know the surface is not hidden, on the basis of Pluto's strong lightcurve amplitude, leaving replenishment as the preferred mechanism for keeping Pluto bright. Such replenishment could either come from an active interior or the annual atmospheric volatile transport cycle. It was then argued that Pluto's secular dimming since 1955 would naturally result from the exposure of an underlying layer of dark CH_4 photochemical products by the sublimation of a bright, thin CH_4 veneer as the planet approached perihelion. Based on this chain of reasoning and some quantitative modeling, Stern et al predicted the presence of a CH_4 atmosphere with a lower limit of 16–45 cm-am column abundance.

These two, essentially theoretical arguments are sound. However, they do not carry the same weight as a positive, direct atmospheric detection. Unfortunately, a definitive detection proved to be extremely difficult.

During the period 1970–1980, various groups searched for a blue upturn in Pluto's near-UV spectrum, which would be indicative of atmospheric Rayleigh scattering. Initially Fix et al (1970) reported such an upturn below 3800 Å, indicating the possible presence of a substantial atmosphere. It was this report that led Hart (1974) and Golitsyn (1975) to speculate about massive, noble gas envelopes surrounding Pluto. However, Barker et al (1980) convincingly showed that previous indications of a Rayleigh

signature were erroneous. In retrospect, it is now clear that the search for a blue upturn was in vain. This is because the mutual events have now demonstrated that Pluto's albedo is high, making its surface cold ($T < 50$ K), so that virtually no frost (except perhaps neon or argon) could generate sufficient vapor pressure in equilibrium with the surface ices to support the tens of millibars required to generate a detectable signature (i.e. a few percent blue upturn).

The greatest difficulty in proving Pluto has an atmosphere, however surprisingly, came from uncertainties in the interpretation of the easily-detectable CH_4 absorption bands in Pluto's spectrum. This is due to the uncertainty in the relative contributions of methane gas and ice in the formation (and for the strongest bands, saturation) of various red and near-IR methane absorption bands. In the period 1978–1987, numerous investigator teams attacked this problem (Benner et al 1978, Fink et al 1980, Cruikshank & Silvaggio 1980, Barker et al 1980, Apt et al 1983, Buie & Fink 1987), with surprisingly little agreement. Aptly, Cruikshank (1990) summarizes the chronology of this debate, which I will not dwell on long.

In essence, the difficulty was due to the fact that no gaseous CH_4 absorption spectra made at P, T conditions expected on Pluto were available. Although it might seem such a situation could be remedied easily, the laboratory preparation of methane gas at temperatures below the CH_4 freezing and melting points makes such a quest problematic. Thus, investigators were left applying corrections for thermal and pressure effects to CH_4 absorption spectra made under significantly different conditions than those expected at Pluto, resulting in uncertainties. This allowed different groups to conclude that most (Benner et al 1978 and Fink et al 1980 who preferred $\sim$27 m-am of gas), some (Barker et al 1980 who preferred $\sim$1–3 m-am of gas and Buie & Fink who preferred 5.5 m-am of gas), or virtually none (Cruikshank & Silvaggio 1980, Apt et al 1983) of the CH_4 bands were due to an atmosphere.

It was hoped these differing interpretations could be resolved by searching for variations in the CH_4 bands with rotational phase, in order to determine whether or not their depths were correlated with albedo changes. Presumably, if the vapor-dominant models were correct, there would be little correlation. However, Buie & Fink (1983) and Cruikshank et al (1985) reported direct albedo/methane-absorption correlations (minimum absorption at minimum light; cf Section 5), but Sawyer et al (1987) claimed no such correlation. [Today there are additional data supporting the positive lightcurve/methane-absorption correlation (Marcialis & Lebofsky 1991, Spencer et al 1990).]

Circumstantial evidence regarding the atmosphere was reported from

thermal-IR flux measurements made by the *IRAS* satellite. Three analyses of *IRAS* measurements were reported (Tedesco et al 1987, Aumann & Walker 1987, Sykes et al 1987). *IRAS* clearly detected the unresolved Pluto-Charon binary at 60 and 100 μ, and made a very marginal detection at 25 μ. Tedesco et al's (1987) paper was essentially restricted to modeling the radii of Pluto and Charon, and will not be discussed further here. Aumann & Walker found the standard thermal model for asteroids (Morrison 1973) to be sufficient to fit the data, with possible surface temperatures of 45–58 K. As such, they claimed that Pluto was warm enough to support a CH_4 atmosphere of 6.7 cm-am to 27 m-am. Sykes et al (1987), however, argued that the standard thermal model does not apply in the cryogenic, outer Solar System. They therefore modified the model to account for both IR beaming and latitudinal surface thermal gradients. From the refined model, they found Pluto cannot be fit to an isothermal surface model, as Trafton & Stern (1983) suggested would be obtained from a substantial atmosphere over a spherical planet. Sykes et al thus predicted an upper limit column of 9.4 m-am CH_4, and a surface albedo distribution best fit by a very dark equatorial band (with $T = 58.2 \pm 0.9$ K), and two bright polar caps ($T = 53.4 \pm 0.8$ K).

In addition to the *IRAS* results, a single report of a radio-wavelength detection of Pluto+Charon at 1.2 mm has been given by Altenhoff et al (1988). These workers found Pluto's skin temperature to correspond to 31–39 K, a surprisingly low value which begs for confirmation or correction. Such a low temperature corresponds to a negligible methane column.

Unfortunately, the mm-wave and *IRAS* thermal-IR results are each dependent on model parameters (e.g. the surface emissivity) that are unknown, leaving them, like the other data described above, weak substitutes for the actual detection of a clear atmospheric signature. However, the definitive atmospheric detection experiment soon came, on June 9, 1988, when Pluto's tiny disk occulted a 12th magnitude star.

7.2 *The 1988 Occultation*

Several attempts to observe stellar occultations of Pluto occurred prior to the 1988 event. Halliday et al (1966) reported observations of a 1965 near-miss which constrained Pluto's radius to <6500 km, but was of course unable to yield information on the atmosphere. Walker's (1980) stellar occultation of Charon was another such event. Later, in 1985, Brosch & Mendelson (1985) observed what they claim is a grazing occultation showing evidence for an atmosphere; however, these data were taken during a period of intense overhead Israeli-Jordanian aerial combat, and have never been published.

The June 1988 event had been predicted several years in advance (Mink & Klemola 1985). This event was a good candidate for several reasons, including (*a*) the star was bright (12th magnitude), thereby offering for good S/N, (*b*) Charon was near elongation and well removed, and (*c*) the event occurred near the zenith on a major landmass. Careful astrometry in the months and weeks leading up to the event was instrumental in properly deploying resources near and along the predicted shadow path.

Photometric observations of the occultation were reported by eight groups stationed in (and over) the South Pacific and Australia; one of these eight, led by J. Elliot, observed the event from the 0.9-m telescope aboard the Kuiper Airborne Observatory, 12.5 km over the ocean.

The most basic, immediate, and well agreed upon result of the occultation was the discovery by all observers that the star dimmed gradually, rather than abruptly. This signature (see Figure 5, *top panel*) is characteristic of differential atmospheric refraction (cf Baum & Code 1953), and serves as definitive evidence for Pluto's atmosphere.

To further interpret the Pluto occultation lightcurves, it is necessary to generalize the standard lightcurve analysis algorithm to include effects of limb curvature and the fact that Pluto's atmosphere is, as had been predicted (cf Section 7.3), comparable in radial extent to the planetary radius. Elliot et al (1989) and Hubbard et al (1989) made such corrections. Both groups assumed a standard isothermal atmosphere for their analyses.

Elliot et al found the half-light level of the KAO lightcurve to occur at 1214 ± 20 km; at this altitude they derived a scale height of 59.7 ± 1.5 km and a temperature to mean molecular weight ratio $T/\mu = 4.2 \pm 0.4$ K/amu. Assuming Pluto's atmosphere is pure CH_4 (the simplest interpretation), these results imply a temperature of $T = 67$ K, a number density $n = 8.3 \times 10^{13}$ cm^{-3}, and a pressure of $P = 0.78$ microbars at the half-light level.

Hubbard et al (1989) analyzed the Hobart Australia lightcurve and found similar results, with a scale height of 46–57 km at a half-height level of 1240 km from Pluto's center. They estimate that this level corresponds to an altitude near 125 km for a warm (61 K) isothermal atmosphere and 175 km for a cold-case (50 K) isothermal atmosphere. A number density of $n = 8 \times 10^{13}$ cm^{-3} was found at the half-height level. Hubbard et al (1989) [and Hunten et al (1988) in a previous, brief report] also pointed out the important conclusion that because (*a*) the occultation track they actually observed was outside the shadow of the planet, and (*b*) the occultation was observed at altitudes ≈ 1000 km over the planet, one could determine that Pluto's atmosphere is indeed widely distended, as various workers (e.g. Trafton 1980, Hunten & Watson 1982, Trafton et al 1988a) had predicted.

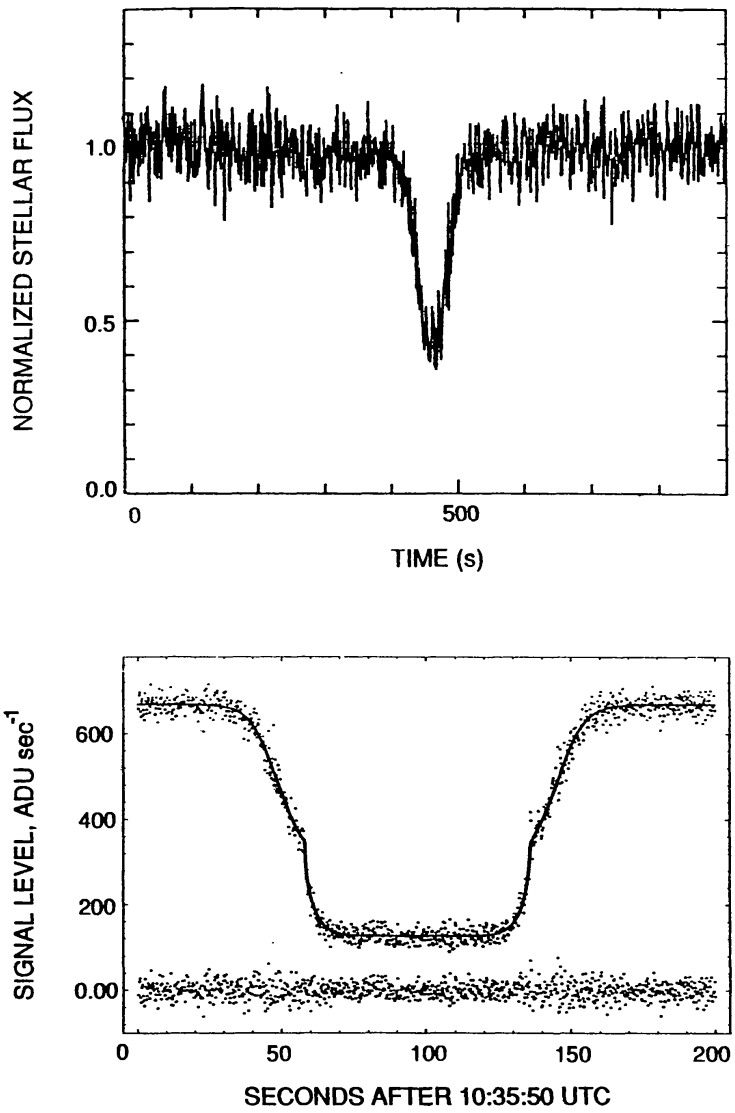

Figure 5 Top panel shows the June 9 1988 occultation of Pluto by a 12th-magnitude star viewed from Hobart, Australia (adapted from Hubbard et al 1989). Bottom panel is the KAO lightcurve and a fit to it (adapted from Elliot & Young 1992). Residuals to the model fit are the points along the bottom; this lightcurve shows the distinct slope steepening which has led to the discussion of haze layers and thermal gradients in Pluto's atmosphere. The time scales in the two panels are not referenced to the same zero point.

We thus see that the broad results of these occultation measurements were similar. Interestingly, they imply a column substantially less than 1 m-am, indicating that the CH_4 bands observed in Pluto's spectrum are essentially all surface-generated. In one very important respect, however, the occultation lightcurves differed strongly, with important implications.

Figure 5 (*bottom panel*) shows the KAO occultation lightcurve. The

important attribute of this lightcurve which distinguishes it from the others is the sudden and persistent steepening that occurs at about the 40% light level. This steepening causes the minimum light level to be more than 2.5 times lower than would be predicted on the basis of an isothermal, clear-atmosphere fit to the lightcurve above this point. Elliot et al (1989) interpreted this steepening as the result of an aerosol or dusty haze layer imbedded in the isothermal atmosphere with a sharp upper boundary lying 25 km below the half-light level (i.e. 1189 km from the center of Pluto). This model exhibits a haze scale height of 33.4 ± 6.9 km, and a normal optical depth $\tau = 0.19$. [As an interesting aside, it is worthwhile to note that water-ice extinction layers called polar mesospheric or noctilucent clouds form from meteoritic water condensing on dust near the Earth's summer mesopause, which is a similar P, T environment to the half-height occultation light level in Pluto's atmosphere. However, these clouds are very thin ($\tau \approx 10^{-3}$) compared to the extinction layer proposed by Elliot et al.]

Beyond the obvious atmospheric consequences of the haze interpretation, the Elliot et al model also introduces uncertainty in the actual amplitude of Pluto's surface lightcurve and whether the mutual event lightcurves are actually detecting the surface radius of Pluto, or simply some larger, "photometric" radius induced by the haze. According to Elliot et al (1989) and Elliot & Young (1991b), Pluto's radius could plausibly be 100–150 km different from the 1150 km value derived from the mutual events (Tholen & Buie 1990).

The most natural source of atmospheric haze would be a photochemical aerosol layer produced by the action of sunlight on methane. Elliot et al discussed the fact that since the extinction scale height is about half that of the clear atmosphere at this level (as extrapolated from the half-height level), this could provide a means of constraining the haze production mechanism—but no definitive constraints were obtained.

Stansberry et al (1989) criticized the haze interpretation on the grounds that the conditions necessary to reproduce the optical depths observed by Elliot et al (1989) require both twice the haze mass production rate expected from sunlight acting on Pluto's methane atmosphere, and haze particulates that are an order of magnitude more absorbing in the visual than are Titan's aerosols. Stansberry et al thus concluded that either (*a*) Pluto's photochemical haze production rate and scattering characteristics are unique in the outer Solar System, (*b*) that the extinction is caused by some other source (such as ground fogs), or (*c*) that the occultation lightcurve was steepened by temperature gradients, rather than hazes.

The alternative suggestion of a thermal gradient was first made by Eshleman (1989), and shortly thereafter by Yelle & Lunine (1989). Hubbard et al (1989) showed the lightcurve steepening to be a natural result

of a thermal gradient. Eshleman's suggestion was that a temperature inversion in a thin boundary layer could produce the lightcurve steepening at Pluto, in analogy to steepenings of radio occultation profiles at Mars and Uranus. Eshleman (1989) also pointed out that if his scenario is correct, then the occultation probed into the boundary layer. This in turn implies the KAO occultation virtually reached the solid surface, which would be at a radius very close to the mutual event solution (Tholen & Buie 1990), rather than far below it (as suggested by Elliot et al 1989).

Yelle & Lunine (1989) constructed a first-order model which assumed methane's 3.3 μ absorption and 7.8 μ emission dominate Pluto's atmospheric radiative balance. Their model indicates that the atmospheric radiative/conductive balance, over a wide range of mixing ratios down to 0.1% methane, would cause the atmospheric thermal profile to reach 101–106 K a few tens of km above the surface, at the 1 μbar level. Above this altitude, their model predicts an isothermal profile. Adopting this vertical thermal profile and the occultation-derived scale-height quotient $T/\mu = 4.2 \pm 0.4$ K/amu, Yelle & Lunine find a mean atmospheric molecular weight of $\bar{\mu} = 25 \pm 3$ which implies the presence of a second, heavier gas in substantial mixing ratio (i.e. 40–65%) with the methane. Based on volatility and cosmochemical arguments, Yelle & Lunine suggest the heavier, second component could be CO, N_2, or Ar, with CO preferred. Other workers had previously suggested Pluto may have a second, heavier gas in its atmosphere, though the preference for CO is not universal. Indeed, with Triton's atmosphere dominated by N_2, a CO-dominated atmosphere at Pluto would be intriguing, at the least.

Owing to the much higher vapor pressures of their second-gas candidates, the Yelle & Lunine model predicts the second gas is highly undersaturated. It would therefore have to be either released in small quantities from the interior or present in a very dilute (1–0.1%) surface-mixture, or in scattered, ponded reservoirs on the surface. Why such a situation might occur is unclear (though it provides interesting grist for thought).

Hubbard et al (1990) extended the analysis of Yelle & Lunine to show that the Yelle & Lunine CH_4-dominated radiative balance model could reproduce the structure of the occultation lightcurve by adopting a near-surface temperature profile with a gradient of about 10 K/km, joining the 106 K high-altitude isotherm at the level of the lightcurve steepening. Still, however, this later model does not reproduce the very low light level at the bottom of the KAO occultation profile, indicating that some combination of a steepening boundary layer profile and a thin, near-surface extinction layer may be required. If the thermal gradient model is correct, it also implies that Pluto's radius is larger than the mutual event-derived values, perhaps by 50–60 km.

Elliot & Young (1991b) recently reanalyzed the KAO lightcurve with a more complete physical model and a larger range of test hypotheses. Based on this reanalysis, they improved their original fit parameters to $T = 60 \pm 12$ K, $n = 5.9 \pm 1.1 \times 10^{13}$ cm^{-3}, and $P = 0.49 \pm 0.14$ μbar, corresponding to a half-height column abundance of $N = 13.4 \pm 2.8$ cm-am for a pure CH_4 atmosphere. If Pluto's atmosphere is predominantly N_2 (as is Triton's), Elliot & Young report their data correspond to a temperature of 104 ± 21 K, with $n = 8.8 \pm 1.6 \times 10^{13}$ cm^{-3} and $P = 1.26 \pm 0.35$ μbar, for a column abundance of $N = 19.8 \pm 4.1$ cm-am at the half-height level. Further, Elliot & Young extrapolated the KAO half-height parameters to the surface for the case of a clear isothermal atmosphere under different compositional assumptions (pure CH_4, pure N_2, pure CO, and a 50/50 Ar/CH_4 mixture). From this, they predict total surface column abundances of 21–39 cm-am, with corresponding pressures of 0.8–2.5 μbar, depending upon the composition.

They also allowed the high-altitude portion of the profile above the half-height level to be fit with the atmospheric temperature gradient as a free parameter. They found their data implies an isothermal high-altitude atmosphere hundreds of km above Pluto's surface, which is consistent with the methane radiative balance model. Elliot & Young do not, however, agree that the occultation profile in the lower atmosphere must be caused by CH_4 radiative balance, and still believe the extinction hypothesis is a viable mechanism for producing the low-altitude lightcurve steepening.

Thus, as of late 1991, the haze/thermal gradient question remains open. Clearly, a haze layer can explain the steepening occultation lightcurve, however, its presence appears ad hoc and its characteristics appear unrealistic. Similarly, a thermally-dominated CH_4 atmosphere will produce a near-surface thermal gradient and a warm stratosphere that could be responsible for the lightcurve steepening. However, Pluto's atmosphere is certainly not purely methane, since at least the photochemical products of CH_4 itself are present. Several of these minor species (e.g. C_2H_2) are efficient radiators which can severely perturb the thermal structure of the atmosphere. Because the haze/thermal gradient issue is open, so too are both the bulk composition and the mixing ratio of CH_4. As with Triton during the *Voyager* encounter, CH_4 could be only a trace constituent.

To resolve the cause behind the steepening of the KAO occultation lightcurve, better models and new data are required. One important model improvement would be a coupled photochemical/radiative code. An important new observational test would be an ultraviolet spectroscopic search for various N- and O-bearing species in Pluto's atmosphere, includ-

ing of course, CO. Beyond their importance to atmospheric studies, such detections would also give important clues to Pluto's internal composition and cosmochemical origin. For species detected both in absorption (over a bright disk) and in emission (in the extended atmosphere), such detections could also constrain the high-altitude vertical structure of the atmosphere, with important implications for escape models (cf Section 7.3). A second observational test would be the simultaneous visible/IR observation of a future occultation (Mink et al 1991), which could distinguish between aerosols (which should not affect the profile at IR wavelengths) and a clear atmosphere with a steep thermal gradient.

7.3 *Atmospheric Models: Dynamics, Escape, and Chemistry*

Trafton & Stern (1983) and Stern & Trafton (1984) performed early studies of Pluto's atmospheric dynamics. However, the rush of results from the 1980s has left much of this work appearing quaintly out of date. By making simple corrections for our present-day understanding of Pluto's bulk parameters and total atmospheric pressure (about an order of magnitude less than believed in the early 1980s), however, one can still draw useful conclusions from this work. Among these are: 1. that very strong seasonal (and perhaps even some diurnal) effects should occur; 2. that as Pluto moves away from perihelion and toward its solstice, the atmosphere should drop precipitously in bulk, perhaps becoming localized over the illuminated hemisphere once the column drops below ≈ 4 cm-am; 3. that the mixing ratio of any more volatile constituent than CH_4 (e.g. N_2, CO, or Ar) will increase when the methane selectively condenses out as Pluto diurnally or seasonally cools; 4. that around perihelion, Pluto's atmosphere may display meteorology driven by baroclinic instabilities, but that a simpler symmetric circulation regime is expected away from perihelion; and 5. that tidal effects due to Charon are expected to be small—at most a few percent.

The escape of gases from Pluto's atmosphere has been studied by several groups. In very early work, Trafton (1980) modeled escape from an isothermal atmosphere and concluded (*a*) that rapid hydrodynamic escape should be occurring which (*b*) would cause Pluto to lose all volatiles in contact with the surface, unless some heavier gas (e.g. Ar) provided a diffusive escape barrier. However, Hunten & Watson (1982) showed that this would not occur because escape-induced adiabatic cooling invalidates the isothermal atmosphere assumption, inducing a throttle on the ability of EUV-driven energy deposition to drive escape. Solving for the energy-limited hydrodynamic escape rate, Hunten & Watson (1982) in fact found it unlikely that more than a few km of CH_4 ice could have been lost since

the beginning of the Solar System, and that the maximum, energy-limited escape flux would be near 4×10^{10} cm^{-2} sec^{-1}.

Trafton et al (1988) employed the Hunten & Watson model (itself based on Watson et al 1981) and improved bulk parameters from the early mutual events to confirm that Pluto would lose at most a few percent of its mass to hydrodynamic escape; they found an orbitally-averaged nominal escape flux of 2.1×10^{10} cm^{-2} s^{-1} (referred to the surface) for a pure-CH_4 atmosphere. They also found only marginally ($\sim$2 times) higher escape rates if heavier species like N_2 or CO dominate the atmosphere. Hubbard et al (1990) then extended escape work by using their occultation-derived thermal profile to find an upper limit to the perihelion CH_4 escape flux of 6×10^{10} cm^{-2}, depending on whether the escape is controlled by the thermal structure below it (as in the Watson et al formalism), or above it (as in Parker's solar wind formalism). In fact, Hubbard et al (1990) found the escape rate to be more sensitive to the thermal structure above it (where EUV is deposited), rather than below it. This situation is analogous to Parker's stellar coronal theory.

McNutt (1989) then examined hydrodynamic escape with an analytic model. He employed this model and the results of the stellar occultation to find that the escape rate could be some 5 times lower than Trafton et al (1988) and Hubbard et al (1990) predicted, if the cooler, Elliot et al (1989) atmosphere is real, and perhaps 10 times lower still if the role of EUV heating in Pluto's upper atmosphere is small. Like Trafton et al (1988), McNutt found that CO or N_2 atmospheres would suffer escape rates only $\sim$2 times as high as a CH_4-dominated atmosphere (for the same thermal profile).

In yet another model, Trafton et al (1987) directly integrated the hydrodynamic equations, so that some of the approximations needed to derive an analytic upper limit solution were not required. Using the output of this model as a boundary condition at the level where collisions become rare ($\sim 4.6\ R_{pl}$, $n \approx 10^6$ cm^{-3}), Whipple et al (1989) then integrated molecular orbits in the restricted three-body formalism to determine the shape and extent of Pluto's distant, outer atmosphere. They found the atmosphere would be highly extended, so much so that (ignoring perturbations by Charon), the number density at Charon's orbit for a pure-methane case was found to be $10^3 < n < 10^4$ cm^{-3}, with the vast majority (86%) of the particles still bound to the Pluto-Charon system. These surprising results indicate Pluto's exosphere may be so distended that it resembles a cometary coma in some respects. Whipple et al (1989) also found that direct transfer of gas from Pluto to Charon occurs over a Roche lobe, but speculated that Charon's weak gravity will prevent the permanent buildup of accreted volatiles. One eagerly awaits observational detection of this extended

envelope, and perhaps, even the detection of the Roche lobe and/or tail structure in it.

Most recently, Clarke et al (1992) examined the consequences of CH_4 photodissociation in this extended envelope and predicted a substantial H/H_2 corona to result. In their model, H column densities exceeding 3×10^{15} cm^{-2} at impact parameters up to several tens of R_{pl} are possible, though a wide range of uncertainty exists. The predicted columns are more sensitive to the escape rate than to the atmospheric CH_4 mixing ratio. Clarke et al also report the (relatively unconstraining) 70 Rayleigh non-detection of H Lyα by *IUE* (limited by the interplanetary H Lyα foreground). They suggest a UV echelle spectrograph may be able to detect the H corona.

We thus see that although Trafton's initial suggestion that hydrodynamic escape would be so rapid as to evaporate Pluto was incorrect, he was correct in pointing out that Pluto's low mass is conducive to hydrodynamic escape. Indeed, Pluto is probably the only planet in our solar system undergoing significant hydrodynamic escape in the present epoch. It is interesting to note that Pluto's atmospheric escape rate varies on two important timescales. The first is the orbital timescale, on which both the atmospheric column and EUV heating change. The second is the 11-year solar cycle, which causes the EUV input to Pluto's atmosphere to change by almost as much as it does when Pluto moves from perihelion to aphelion. These factors make Pluto a unique laboratory for atmospheric science, with potential relation to hydrodynamic escape models for the early terrestrial planets.

Finally, it is worthwhile to remark on the dearth of aeronomical modeling at Pluto: No published studies of the chemistry of either pure CH_4 or $CH_4/N_2/CO$ atmospheres at Pluto have ever been reported. Such studies might lead to important insights about surface composition, and the presence of potentially detectable trace species (e.g. CN) diagnostic to the atmosphere's full composition and key physical properties.

7.4 *Atmosphere/Solar Wind Interaction*

Bagenal & McNutt (1989) have recently undertaken a first-look at Pluto's atmospheric interaction with the solar wind based on present-day knowledge of the atmospheric structure and characteristics. This study found that if Pluto has no strong intrinsic magnetic moment and its atmospheric escape rate is low (i.e. $< 1.5 \times 10^{27}$ s^{-1}, as expected if Pluto's upper atmosphere is cool, or if EUV deposition is inefficient), then Pluto's solar wind interaction will be Venus-like. In this situation, Pluto's ionosphere will act as a barrier, standing off both the interplanetary magnetic field and charged particle penetration. If the escape rate exceeds this value, however, they

find Pluto's solar wind interaction will be comet-like, with extensive upstream ion pickup and consequent mass loading of the solar wind. Figure 6 illustrates both cases. In either case, the size of Pluto's solar wind interaction region can vary (due to changing solar wind conditions) from 3 to 30 Pluto radii in scale on timescales of days. Apparently, Charon is sometimes outside and sometimes inside the solar wind interaction region.

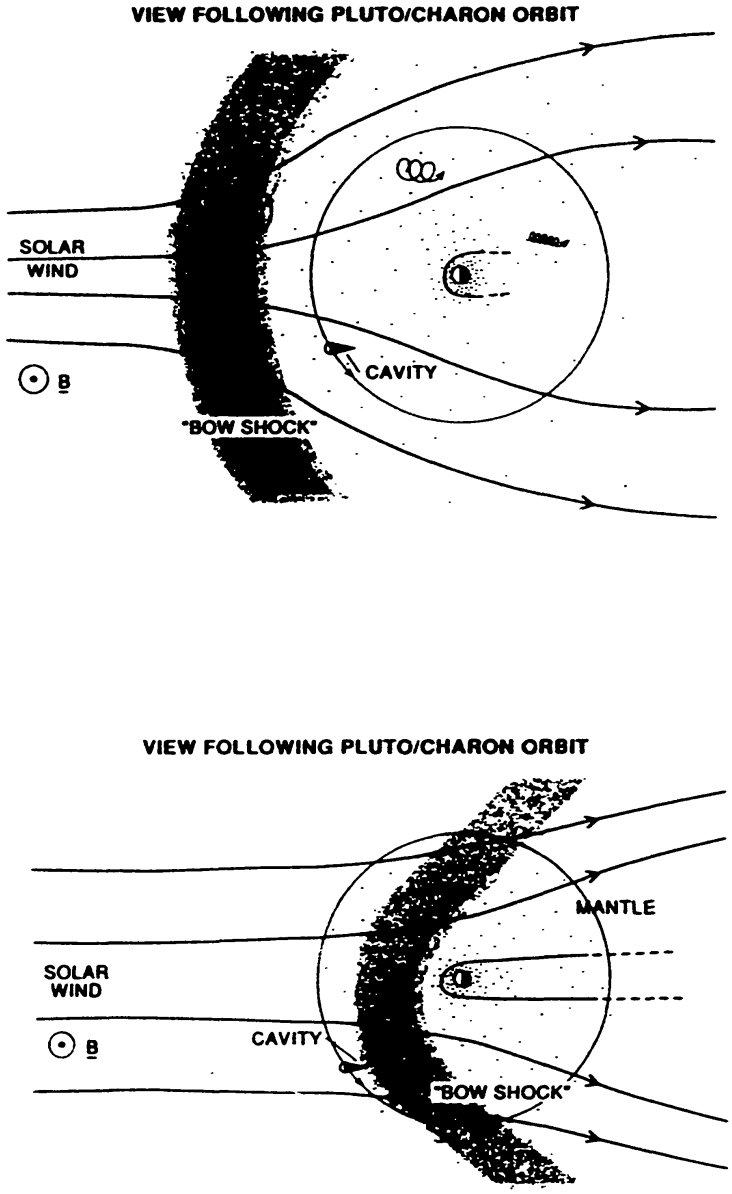

Figure 6 A sketch of the interaction between Pluto and the solar wind for the case of strong (*top panel*) and weak (*bottom panel*) atmospheric escape. Charon's orbit is shown for reference. Adapted from Bagenal & McNutt (1989).

Bagenal & McNutt point out to future investigators that because the scale-length of the interaction region is comparable to the predicted thickness of the upstream shock, a fully kinetic treatment is required for more detailed solar wind interaction studies.

7.5 *Volatile Transport*

Pluto's high obliquity and the spectral evidence for methane attest to the present ubiquity of volatiles on the surface. Yet, over the lifetime of the Solar System, escape models imply that Pluto has lost its atmosphere 5×10^4–5×10^5 times. Clearly, a substantial volatile reservoir must exist on or near the surface if the atmosphere is to be continuously replenished.

Prior to the 1988 occultation, Stern et al (1988) examined the implications of Pluto's high albedo in the presence of solar UV and Galactic cosmic ray (GCR) radiation. Such radiation causes surface ices to darken and atmospheric methane to be photochemically converted to C_2 and C_3 hydrocarbons (or nitriles if nitrogen is present in bulk). They estimated that ~ 300 g cm^{-2} of dark methane-photochemical products have been created or deposited on Pluto's surface over the past 4.5×10^9 years. Stansberry et al (1989) found comparable or higher rates of deposition from aerosol haze production.

From the fact that Pluto is indeed bright, Stern et al concluded that Pluto must have an atmosphere that annually "launders" the surface. According to their model, seasonal cycles on Pluto proceed as follows: At aphelion, Pluto is so cold that the atmospheric mass is greatly reduced, through condensation, and the atmosphere is almost entirely lying on the surface as a fresh, bright frost. The total atmospheric column corresponding to the 1.5 μbar surface pressure only corresponds to a few tenths of a g cm^{-2} of frost. This fresh frost, if left exposed, would be converted to dark hydrocarbons on a timescale of a few hundred orbits. Johnson (1989) found an even faster darkening time: a few to perhaps ten orbits. As perihelion approaches, increasing insolation causes the surface frosts to sublime, recreating the atmosphere but leaving behind the involatile, carbonaceous photochemical products. The removal of this layer during the approach to perihelion would then explain the secular decrease in Pluto's albedo since the mid-1950s (Hardie 1965, Marcialis 1983).

This model predicts that after perihelion volatile transport will cause Pluto to brighten and exhibit a decreasing lightcurve amplitude as it cools and the atmosphere is again deposited as a clean frost on the surface (of course, properly distributed fixed albedo spots can do this as well). It also predicts that the dark areas found from surface-spot models may be the places where all the frost has already sublimed (the fact that the dark spots are now known to correlate with CH_4-depleted areas supports this), and

that *HST* (at spec resolution) will be able to detect time-variable changes in Pluto's albedo pattern over the next 10–15 years.

Recently, Trafton (1990) modeled the seasonal effects of a generic, two-component volatile atmosphere on Pluto, showing that although the atmospheric composition can yield information on the relative volatile fractions in the bulk interior reservoir, the surface ice volatile fractions may not be representative of the interior.

Going back in time, Binzel (1990) has suggested that the volatile transport scenario extends to the much longer (i.e. 3.7×10^6 yr) timescale induced by the precession of Pluto's perihelion. According to this work, Pluto's bright southern polar cap is the result of a long-term net flow of condensing methane to that hemisphere (which is in shadow) as Pluto draws away from perihelion. As such, over the 3.7×10^6 yr obliquity period, the two poles reverse roles as the net volatile sink, and therefore reverse roles as the brightest cap. If true, then flyby imaging of these regions might detect Mars-like polar layered terrain showing evidence for these long-term seasonal cycles.

8. CHARON: SURFACE, INTERIOR, AND ATMOSPHERE

Because Charon is much dimmer than Pluto and is so close to it as seen from Earth, it is very hard to study. Indeed, it can be said that without the mutual events, occultations, or *HST* to separate the Pluto and Charon signals, Charon would remain virtually a complete unknown. This section collects all of the available information on Charon's physical characteristics, except its radius, which was described in Section 4, and its orbit which was described in Section 3. Comments on possible origin scenarios will be described in Section 9.

8.1 *Photometric Properties and Surface Composition*

Data on Charon's photometric properties and surface composition have come from both conventional techniques and mutual event photometry and spectrophotometry. Each is discussed in turn.

A few nonmutual event observations of the Pluto-Charon system have yielded useful data on Charon's photometric properties. In an early report, Reitsema et al (1983) made *V*-filter CCD observations in good seeing when Charon was near greatest northern elongation from Pluto in 1980. These workers derived a Pluto:Charon brightness ratio of 5.5:1. If we use mutual event-derived radii to convert this brightness ratio to relative albedos, we find they imply an expected albedo ratio of Pluto to Charon

of 1.5:1. Knowing Pluto's albedo on the hemisphere viewed by Reitsema et al as a result of the mutual event-derived lightcurves, one can derive a geometric albedo for Charon of $p_{ch} = 0.31$ when it is at northern elongation. Although this simple estimate neglects possible changes on Pluto between the 1980 Reitsema observations and the 1986–1988 mutual event measurements of Pluto's albedo, and assumes Pluto and Charon's phase laws are identical, it does give us an approximate albedo for a Charon hemisphere that could not be directly sampled by the mutual events.

Jones et al (1988) later reported multicolor *B*- and *I*-band filter CCD observations in sub-arc second seeing at CFHT. These observations, made on June 17–18, 1987 were made near southern elongation (0.5 rotational phase). Jones et al then used early mutual event radii of 1148 and 613 km for Pluto and Charon, and, through careful fitting and removal of Pluto's contribution to their images, found geometric albedos. In the *B* band they found $p_{pl} = 0.546 \pm 0.029$ and $p_{ch} = 0.318 \pm 0.034$. In the *I* band they found $p_{pl} = 0.726 \pm 0.039$ and $p_{ch} = 0.372 \pm 0.021$. As indicated in their paper, these data indicate that on the hemisphere they observed, Charon is darker and more neutrally colored than Pluto.

Charon's (relatively) low albedo and grey color indicates a widespread contaminant in the surface water ice. Trafton et al (1988) have suggested that the byproducts of CH_4 photochemistry in an ancient Charonian atmosphere could produce such a residue. However, whether such an atmosphere ever existed, and even whether Charon's surface contaminant is silicious or carbonaceous remains unknown.

Other information on Charon's albedo and possible lightcurve has come from the mutual events themselves, most particularly the mid-season events in 1987 and 1988 in which Charon completely disappeared behind Pluto. By subtracting system (i.e. Pluto+Charon) photometry or spectra made just prior to such events with Pluto-only spectra made during totality, various investigators have been able to generate Charon-only albedos, colors, and even moderately-good S/N spectra. Although this provides a valuable window on Charon, one must keep in mind this window is only open at the rotational phase of the inferior events, ≈ 0.75.

Binzel (1988) employed just such events (on April 4 and May 22, 1987) to derive Charon's $B-V$ color on its eclipsed hemisphere, and an upper limit to the hemispheric color variation between this hemisphere and its opposite. Binzel found $B-V = 0.700 \pm 0.001$ on the eclipsed hemisphere, and a $<5\%$ 1σ variation between this hemisphere and its opposite, derived from *B* and *V* measurements during a superior event.

As shown in Figure 7 (*top panel*), Fink & DiSanti (1988) reported a

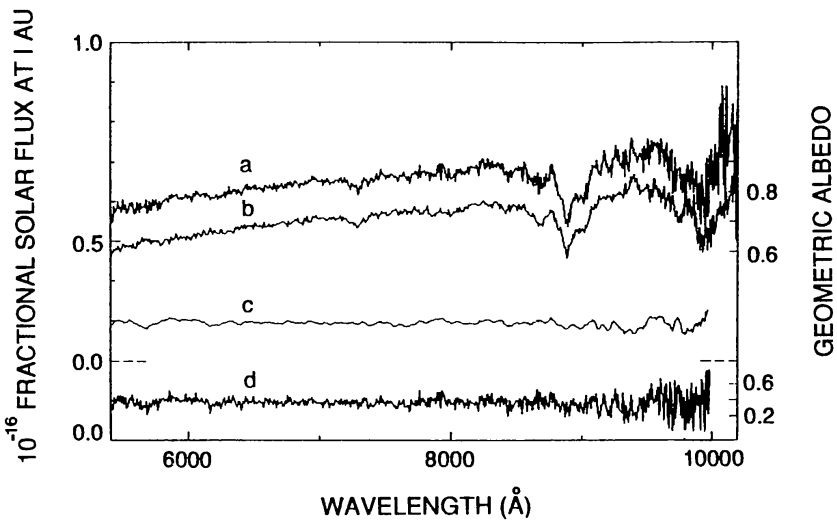

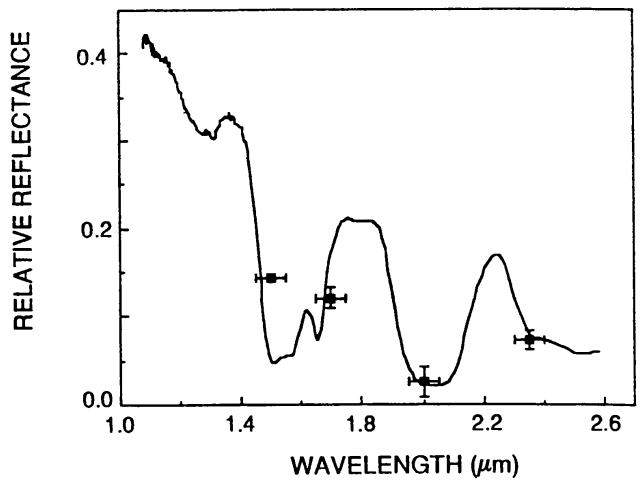

Figure 7 Pluto and Charon spectra. Top panel shows spectra of: (*a*) Pluto+Charon made prior to eclipse; (*b*) Pluto-only after second contact with Charon hidden; (*c*) Charon-only smoothed to 80 Å resolution resulting from the subtraction of (*a*)−(*b*); and (*d*) the raw Charon-only spectrum resulting from the subtraction of (*a*)−(*b*). Notice that the strong methane absorption bands present in Pluto's spectrum are not detected in the Charon-only spectrum. [This panel adapted from Fink & DiSanti (1988).] Bottom panel shows Marcialis et al's (1987) detection of water ice in Charon's reflectance spectrum (data points) against a laboratory spectrum of water ice at 55 K; adapted from Marcialis et al (1987).

Charon-only mutual event spectrum spanning the 5500–10,000 Å bandpass. Their data show that Charon displays a nearly flat (or perhaps slightly blue) continuum, with no detectable CH_4 absorption features, and a 5500 Å albedo of 0.36. When adjusted to the more accurate radius used

by Fink & DiSanti, Sawyer et al's (1987) spectrum, obtained during the same, March 3, 1987 mutual event, gives similar results.

Marcialis et al (1987) and Buie et al (1987) each reported the results of mutual event experiments to derive a Charon-only spectrum in the 1–2.5 μ IR. As shown in Figure 7 (*bottom panel*), Charon's infrared spectrum shows the characteristic absorption feature of water ice, but no evidence of the volatile frosts of CH_4, CO_2, H_2S, NH_3, or NH_4HS. The absence of methane is particularly important, since at the nondetection level given for Charon, CH_4 absorption bands only a few percent as strong as Pluto's can be ruled out.

The presence of water ice, rather than methane ice may indicate Charon's surface better preserves ancient topography than Pluto's. This suggests the speculative but interesting possibility that Pluto's surface may harbor only the record of more recent impacts, while Charon's harbors a long-term integrated flux. One awaits a spacecraft mission to learn if this is indeed the case.

Based on the data just reviewed, one concludes Charon's surface albedo, color, and composition are more like those of the major Uranian satellites, than Pluto's. Indeed, Ariel, with a radius of 580 ± 5 km, a geometric albedo of 0.4, very subtle surface color, and strong water-ice absorption bands (cf Cruikshank & Brown 1986) makes a nice first-order model for Charon's photometric appearance.

However, a significant question has come up in the past few years as to whether or not Charon has significant surface markings. Recall that Tholen & Buie (1990) gave a mutual-event derived B albedo for Charon of $p_B = 0.375 \pm 0.018$; this is the average of B albedo at the event phases 0.25 and 0.75. Recall also that the Jones et al data set give $p_B = 0.318 \pm 0.034$ at 0.5 rotational phase, and that Reitsema's data set corresponds to $p_{ch} \approx 0.31 \pm 0.05$ at 0 rotational phase. Based on these data alone, there is a weak indication of B lightcurve variation, such that rotational phases 0.25 and 0.75 are perhaps 10–15% brighter than phases 0 and 0.5. Whether this effect is real, or simply some offset between data sets, or some other observational artifact, is unclear. What is clear, however, is that compared to Pluto's factor of 25% B albedo lightcurve amplitude, Charon's B amplitude is muted.

The reports of Wasserman et al (1988), Millis et al (1989), and Bosh et al (1992) argue for a non-negligible Charonian lightcurve. The first two reports base their findings on astrometry of Pluto-Charon made in support of the 1988 stellar occultation groundtrack prediction (see Section 7.2). Here, broadband astrometric measurements detected a "well-defined oscillation" of the Pluto-Charon system of magnitude 0.06 arcsec, which may result from a combination of barycentric wobble and Charon's lightcurve.

Although the detected wobble was observed to be in phase with Charon's rotation, it was decidedly nonsinusoidal, indicating a significant (but unspecified) lightcurve contribution. A more complete analysis and a full paper is anxiously anticipated from this data set. The Bosh et al (1992) results indicate that Charon is up to 20% variable at 2.2 μ between orbital phases 0.06, 0.42, and 0.95 where their best data were obtained. This work, which used model-resolved IR images of Charon and Pluto appears to suggest the exciting possibility that the strength of the 2 μ H_2O water-ice absorption feature on Charon varies longitudinally. However, it is unsettling that negligible visible lightcurve variations have been found at virtually the same rotational phases.

Thus, the issue of Charon's lightcurve and albedo/compositional variegation becomes even more intriguing. Perhaps the astrometry and IR results can be made consistent with the visible data sets if there is some peculiar color dependence of the lightcurve. However, this seems unlikely since Charon's visible spectrum is virtually without slope. Alternatively, systematic differences between the Reitsema et al (1983), Jones et al (1988), and Binzel (1988) data sets may simply be masking a real variation, or the IR and astrometry results may themselves have problems. More observations are anxiously awaited, particularly astrometric data to derive the barycentric wobble, and measurement of Charon's lightcurve separately from Pluto's at multiple UV and visible wavelengths.

8.2 *Density, Bulk Composition, and Interior Structure*

Based on the detection of water ice, and the similarities in surface albedo and color noted above, it would seem Charon's bulk composition and interior structure might also be like the major Uranian satellites. If this is the case, then one expects a density in the range 1.5–1.7 g cm^{-3}. However, there is as yet no direct constraint or measurement of Charon's density, and only a dynamical upper limit near 2.3 g cm^{-3} (McKinnon 1989a; cf Section 6.1). Still, the "likely" range of Charon densities from 1.5 to 2.3 g cm^{-3} allows it to be substantially more dense and therefore more rock-dominated than the Uranian satellites. There may also be a substantial component (e.g. 3–10%) of volatiles (e.g. CO or CH_4) locked up in Charon's interior. We simply do not know, and must await additional observations.

Charon's differentiation state depends both upon its unknown bulk composition and thermal history. Charon's small size argues more heavily against its differentiation than Pluto's. However, either a dense Charon with high rock content or an ancient energetic event (e.g. an impact with Pluto) could have induced partial or complete differentiation of this small body. Therefore, this issue too remains open until further data become available.

8.3 *The Possibility of Primordial and Present-Day Atmospheres*

The only identified surface constituent on Charon, water ice, is involatile even at Charon's perihelion radiative-equilibrium surface temperature (~45–60 K, depending on the latitude). Therefore, no atmosphere is a priori expected. Related observational constraints come from Fink & DiSanti's (1988) nondetection of CH_4, which led them to conclude that Charon cannot at present have a methane atmosphere with >5% the column abundance of Pluto's (i.e. a few cm-amagats).

However, very recently, Elliot & Young (1991a) have claimed that a reanalysis of Walker's (1980) Charon occultation lightcurve supports the case for a present-day Charonian atmosphere with up to 13 cm-am of methane, or up to 57 cm-am of other gases, with CO, Ne, Ar, Kr, and perhaps Xe being suggested as candidates.

Trafton et al (1988) examined the escape rate from an atmosphere around Charon to investigate whether a primordial atmosphere may have been lost. Using the hydrodynamic escape model described in Section 7.3, they demonstrated that while Charon may have once had a primordial atmosphere, it would have been lost at rates fast enough to have removed more CH_4 (or CO for that matter) than the cosmogonically expected internal supply. This is not to say Charon's interior does not contain volatiles, since they may be locked up deep in the planet, but simply that the surface supply of volatiles has been long exhausted (unless there is internal activity bringing up volatiles from a deep reservoir). Given the unlikely possibility of internal activity on Charon today, it would seem the lack of CH_4 absorptions and Trafton et al's work together argue quite strongly against an atmosphere. Although this casts doubt on an intrinsic source for a present-day Charonian atmosphere, it is possible that Elliot & Young's result can be understood if Charon's gravity causes it to collect escaping gas from Pluto, as suggested by Whipple et al's (1989) theoretical models (cf Section 7.3). However, what is clearly needed is not further theoretical modeling, but a confirmation or rejection of the Elliot & Young result by occultations, UV spectroscopy, or the direct discovery of some subliming voltage on Charon.

9. ORIGIN OF PLUTO, CHARON, AND THE BINARY SYSTEM

Any viable theory of Pluto's origin must provide a self-consistent explanation for the major attributes of the Pluto-Charon system. These include:

1. the existence of the binary's exceptionally low (~6:1) planet:satellite mass ratio;

2. the synchronicity of Pluto's rotation period with Charon's orbit period;
3. Pluto's inclined, elliptical, Neptune-resonant orbit;
4. the high axial obliquity of Pluto's spin axis and Charon's apparent alignment to it;
5. Pluto's small mass ($\sim 10^{-4}$ of Uranus' and Neptune's);
6. Pluto's high rock content—the highest among all the outer planets and their major satellites; and
7. the dichotomous surface compositions of Pluto and Charon.

This formidable list of constraints on origin scenarios is very clearly dominated by Charon's presence and the unique dynamical state of the binary. Therefore, most of the work on Pluto's origin published prior to Charon's discovery will be ignored here. The interested reader will find such a discussion well-presented in Whyte (1980).

9.1 *Origin of the Pluto-Charon Binary*

Two theories have been considered for the origin of the Pluto-Charon binary: rotational fission and mutual capture via an impact between proto-Pluto and proto-Charon. Formation of Pluto and Charon together in a subnebular collapse is not considered realistic because of their small size; that is standard planetary formation theory (e.g. Safronov 1969) suggests bodies in the Pluto and Charon size class formed via solid-body accretion of planetesimals.

The rotational fission hypothesis was examined by Lin (1981) and Mignard (1981). The basis of this work was their early recognition that the specific angular momentum J_{PC} of the system is close to the critical value for fission of fluid objects; $J_{crit} = 0.39$. After the mutual events allowed the determination of accurate radii for Pluto and Charon, it became clear that J_{PC} clearly exceeds 0.39. McKinnon (1989a) analyzed the effect of Charon's density on J_{PC} and found that $J_{PC} > 0.39$ occurs for a tidally evolved Charon whenever $\rho_{ch} > 1.8$ g cm^{-3}. McKinnon also found that if $\rho_{ch} > 2.3$ g cm^{-3}, $J_P > 0.39$ would be obtained unless Charon formed beyond Pluto's Roche limit. Thus, $\rho_{ch} > 2.3$ g cm^{-3} can be interpreted as a plausible upper limit on Charon's density. However, this upper limit is approximate (as McKinnon himself notes) since various factors including differentiation and the formation distance of Charon from Pluto affect it. Resolution of the Pluto/Charon mass ratio should be an important goal for the 1990s.

Given that the Pluto-Charon system very likely has too much angular momentum per unit mass to have been a single body, it seems more likely that Pluto and Charon were created via a mutual, giant collision.

Previous to McKinnon (1989a), an impact origin hypothesis had been suggested by several authors, including McKinnon (1984), A. R. Hilde-

brand (personal communications 1985, 1986), Burns (1986), and Peale (1986). A similar scenario has been proposed for the origin of the Earth-Moon binary, based in part on its relatively high mass ratio (81:1) and specific angular momentum ($J_{E-M} = 0.115$). Interested readers can consult Hartmann & Davis (1975) and the collection in Hartmann et al (1986) for additional background on the origin of the Earth-Moon binary.

In the giant collision theory, Pluto and Charon formed independently by accumulation of planetesimals, and then suffered a random, chance collision which dissipated enough energy to permit binary formation. In one plausible scenario, Charon was re-accreted from a debris disk left in orbit about Pluto after the collision event. Various authors have attempted to determine whether Pluto or Charon would be the denser object after such a collision. However, no definitive prediction can result from such analysis, because neither momentum nor mass was conserved.

An important qualititative difference between the Pluto-Charon and Earth-Moon giant-impacts is that the relative collision velocities, and hence impact energies of the Pluto-Charon event were much smaller, enormously reducing thermal effects (McKinnon 1989b). Thus, whereas the Earth may have been left molten by the Mars-sized impactor necessary to have created the Moon, the proto-Charon impactor would probably only raise Pluto's global mean temperature no more than 50–75 K. This is insufficient to melt either body, but may have been sufficient to induce either's differentiation. It would have also produced a substantial transient, post-impact, hot, volatile atmosphere with intrinsically high escape rates. Such an escaping atmosphere would have interacted with the Charon-forming orbital debris, fractionating Pluto's present-day volatile content.

This later possibility is particularly interesting because it offers one means for explaining Pluto's high rock content (Simonelli et al 1989). Recall from Section 6 that Pluto's rock (i.e. nonvolatile) fraction is probably close to 70%. This should be contrasted with the near 50:50% rock:ice ratio predicted for objects formed from solar nebula material according to kinetic equilibrium inhibition models and present-day understanding of the nebular C/O ratio (Anders & Grevesse 1989). This high rock fraction indicates that the nebular material from which Pluto formed was CO- rather than CH_4-rich. As such, most of the available nebular oxygen should have gone into CO, rather than H_2O formation, which in turn leads to a high rock:ice ratio. In cosmochemical studies of such scenarios, Lewis & Prinn (1980) find that $CO \rightarrow CH_4$ conversion is inhibited in the cool, low pressure solar nebula, in turn implying rock fractions near 0.7 (Anders & Ebihara 1982). By contrast, rock fractions of ≈ 0.55 are expected in protoplanetary nebulae (Anders & Ebihara 1982) where $CO \rightarrow CH_4$ conversion is not inhibited (Prinn & Fegley 1981). More

recent work by Anders & Grevesse (1989) makes Pluto's rock fraction somewhat higher than solar nebula models would predict. Although this scenario hinges on the solar nebula having been CO-rich, observations of molecular clouds (e.g. Knacke et al 1985) indicate this should be expected.

Thus, McKinnon (1989b) and Simonelli et al (1989) have suggested impact-induced volatile loss may have raised Pluto's density to its present value. McKinnon (1989b) found that hydrodynamic jetting in an oblique impact could remove substantial ice ($\sim$20% of the present-day system mass) if either proto-Pluto or proto-Charon had already differentiated. McKinnon further notes that if Pluto and Charon were formed in a subplanetary nebula, its initial rock fraction would be 35%, and some 50% of the original ice would need to have been removed—an energetically unlikely prospect, which further argues for formation in the solar nebula itself.

9.2 *Pluto's Origin, and Its Implications for the Outer Solar System*

The most widely remembered suggestion for Pluto's origin (Lyttleton 1936) is based on the fact that Pluto's orbit is Neptune-crossing. In Lyttleton's scenario, Pluto was formerly a satellite of Neptune, ejected via a close encounter between itself and the satellite Triton. According to Lyttleton, the encounter also reversed the orbit of Triton. Variants on the "origin-as-a-former-satellite-of-Neptune" hypothesis were proposed by Dormand & Woolfson (1977, 1980), Kuiper (1957), Harrington & Van Flandern (1979), and Farinella et al (1980). However, all of these scenarios were dealt a serious blow by the discovery of Charon, which complicates the already-difficult ejection problem, unless the Pluto-Charon binary formed later, when Pluto was already in heliocentric orbit. Other objections to these scenarios are numerous. First among them is the fact that any object ejected from orbit around Neptune would be Neptune crossing and therefore subject to either accretion or rapid dynamical demise. Further, it is extremely unlikely such an ejected object would be transferred to the observed 3 : 2 Neptune : Pluto resonance. Further still, Pluto is less massive than Triton (by about a factor of two), making it impossible for Pluto to reverse Triton's orbit, and Pluto's rock content is so high that it virtually guarantees that Pluto did not form in a planetary subnebula, even if a Charon impact subsequent to its ejection to solar orbit removed some volatiles.

To summarize, the presence of surface methane on Pluto and water ice on Charon argues strongly for formation in the outer solar system, where ices condense. The relatively high densities and consequent high rock content of these two bodies argues for formation from the solar nebula, rather than from planetary subnebulae material. Following their inde-

pendent formation it would seem Pluto and proto-Charon subsequently collided, forming the binary. This heliocentric formation/collision scenario can account for most of the major attributes of the system, including the elliptical, Neptune-crossing orbit, the high axial obliquities, and the 6:1 mass ratio. Further, Farinella et al (1980) have shown that the present tidal equilibrium state would naturally be reached by Pluto and Charon in 10^8–10^9 years after the binary's formation—a small fraction of the age of the Solar System. The dichotomous surface compositions of Pluto and Charon are a plausible, but not a mandatory result of this scenario. An alternative explanation of the surface dichotomy is Charon's preferential propensity for volatile escape (Trafton et al 1988; see Section 7). In any case, the surface dichotomy is not at odds with the impact scenario.

But if Pluto and Charon did form in heliocentric orbit, why should these two objects, alone in over 10^3 AU^3, "find" each other in order to execute a mutual collision? That is, the impact hypothesis fails to explain (*a*) the existence of Pluto and Charon themselves, (*b*) the very small masses of Pluto and Charon compared to the gas giants in general, and Neptune and Uranus in particular, (*c*) the fact that the collision producing the impact was highly unlikely, and (*d*) the binary's position in the Neptune resonance.

Stern (1991) has suggested the solution to (*a*)–(*c*) lies in the possibility that Pluto and Charon were members of a large population (300–3000) of small ($10^{24.5}$–$10^{25.5}$ g) "ice dwarfs" planets that were present during the accretion of Uranus and Neptune in the 20–30 AU zone. Such a population would make probable the trio of otherwise highly unlikely occurrences in the 20–30 AU region: the impact of Pluto and proto-Charon, the capture of Triton into retrograde orbit, and the tilting of Uranus and Neptune by near-Earth mass bodies. According to this study, the vast majority of the ice dwarfs were scattered (with the comets) to the Oort Cloud and Kuiper Disk by strong perturbations from Neptune and Uranus. Only Pluto-Charon and Triton remain in the 20–30 AU zone today, specifically because they are trapped in unique dynamical niches which protect them against loss to such strong perturbations. Interestingly, it also appears that Pluto's orbital inclination might naturally be explained if it were a moderate outlier in a normally distributed population of ice dwarfs. This is because such a population would naturally induce on itself and small debris in the 20–30 AU equilibrium zone random eccentricities and inclinations of $\langle e \rangle \sim 0.1$–$0.2$ and $\langle i \rangle \sim 5$ deg in a timescale not much longer than the formation and subsequent dynamical clearing time for Uranus and Neptune. An important test for this hypothesis is the prediction that several more (i.e. 3–30) Pluto-Triton-like bodies should exist today in the Kuiper Disk, where they can be detected by photometric or IR techniques.

If this hypothesis is correct, it would imply Pluto, Charon, and Triton are important relics of a very large population of small planets, which by number (but not mass) dominate the planetary population of the Solar System. As such, these three bodies would no longer appear as isolated anomalies in the outer Solar System. Instead they would be genetic relations from a heterogeneous ice dwarf ensemble, and therefore even more worthy of intense study.

10. CONCLUDING REMARKS[2]

The past decade and a half have seen enormous progress in the study of the Pluto-Charon system. In 1975, Pluto's size, mass, and density were each judged to be several times their actual values. In 1975, no hint of their surface compositions or true albedos was available; so too, evidence for Pluto's atmosphere was completely lacking. In 1975, we did not even know that Pluto has a satellite, nor suspect this little world might be intimately tied to understanding the origin of the outer Solar System. Indeed, in 1975 Pluto was often viewed as an oddity with no natural place in the paradigm of solar system formation.

Today, by contrast, we ask detailed questions about Pluto's internal structure and debate its differentiation. The *degree* of volatile transport and the *number* of bulk atmospheric species are important issues. We seek to *measure* Pluto's atmospheric escape rate, atmosphere's thermal structure, and aerosol content. We seek to expand beyond our knowledge of Pluto's gross albedo pattern to determine the correlation between albedo and surface composition. And we look forward to directly measuring the individual masses (and hence deriving the individual densities) of Pluto and Charon.

In just over fifteen years, the techniques available to astronomers studying Pluto have expanded considerably, now including UV and IR spectroscopy, mm-wave detection, and surface mapping. So too, our scientific perspective has been enormously expanded by the detailed *Voyager* reconnaissance of Io and the icy Galilean satellites, Titan and Triton, and over 30 other solid bodies in the outer Solar System.

In the next fifteen years, we look forward to detailed studies of Pluto and Charon by *HST*, *SIRTF*, and *FUSE* from Earth orbit, and by the bevy of new-technology 8- and 10-m class telescopes expecting first light in the 1990s. With these tools, one fully hopes to answer many of our present-day questions, resolve some of the existing controversies, and uncover new mysteries.

[2] As we go to press, T. Owen and coworkers have reported the spectroscopic detection of CO and N_2 ice on Pluto with important implications for Pluto's origin, atmosphere, and relationship to Triton (see *IAU Circ. 5532*, May 1992).

Still, however, we remember the hard lesson taught many times in the space age: Until a planet's surface can be resolved at scales approaching a kilometer, and its atmosphere and solar wind interaction directly sampled, as only space missions can accomplish, one should retain a certain humility and be cautious of unequivocal conclusions. As such, until a spacecraft has reconnoitered the Pluto-Charon system, it will remain, "a puzzle, wrapped in a mystery, itself shrowded in enigma," taunting astronomers against the challenge distance so uniquely enforces.

ACKNOWLEDGMENTS

I thank Dr. Peter Conti for nominating this article for appearance in the *Annual Review of Astronomy and Astrophysics*. I thank M. Buie, A. Dobrovolskis, J. Elliot, R. Gladstone, D. Hunten, R. Marcialis, W. McKinnon, D. Tholen, L. Trafton, R. Yelle, and E. Young for useful critiques of this manuscript. This review is dedicated to the many workers who have contributed to the study of Pluto, and to the memory of Leif Andersson: Had he only lived to see "his" planet's secrets revealed so rapidly in the 1980s!

Literature Cited

Altenhoff, W. J., Chini, R., Hein, H., Kreysa, E., Mezger, P. G., et al. 1988. *Astron. Astrophys.* 190: L15–17
Anders, E., Ebihara, M. 1982. *Geochim. Cosmochim. Acta* 46: 2363–80
Anders, E., Grevesse, N. 1989. *Geochim. Cosmochim. Acta* 53: 197–219
Andersson, L. E. 1978. *Bull. Am. Astron. Soc.* 10: 586 (Abstr.)
Andersson, L. E., Fix, J. D. 1973. *Icarus* 20: 279–83
Appelgate, J. H., Douglas, M. R., Gursel, Y., Sussman, G. J., Wisdom, J. 1986. *Astron. J.* 20: 279–83
Apt, J., Carelton, N. P., MacKay, C. D. 1983. *Ap. J.* 270: 342–50
Aumann, H. H., Walker, R. G. 1987. *Astron. J.* 94: 1088–91
Bagenal, F., McNutt, R. L. 1989. *Geophys. Res. Lett.* 16: 1129–32
Barker, E. S., Cochran, W. D., Cochran, A. L. 1980. *Icarus* 44: 43–51
Baum, W. A., Code, A. D. 1953. *Astron. J.* 58: 102–12
Beletic, J. W., Goody, R. M., Tholen, D. J. 1989. *Icarus* 79: 38–46
Benner, D. C., Fink, U., Cromwell, R. H. 1978. *Icarus* 36: 82–91
Binzel, R. P. 1988. *Science* 241: 1070–72
Binzel, R. P. 1989. *Geophys. Res. Lett.* 16: 1205–8
Binzel, R. P. 1990. *Lunar Planet. Sci. Conf.* XXI: 87–88 (Abstr.)
Binzel, R. P., Mulholland, J. D. 1983. *Astron. J.* 88: 222–25
Binzel, R. P., Mulholland, J. D. 1984. *Astron. J.* 89: 1759–61
Binzel, R. P., Tholen, D. J., Tedesco, E. F., Buratti, B. J., Nelson, R. M. 1985. *Science* 228: 1193–95
Bonneau, D., Foy, R. 1980. *Astron. Astrophys.* 92: L1–4
Bosh, A. S., Young, L. A., Elliot, J. L., Hammel, H. B. 1992. *Icarus* 95. In press
Breger, M., Cochran, W. D. 1982. *Icarus* 49: 120–24
Brosch, N., Mendelson, H. 1985. *IAU Circ. No.* 4097
Brown, G. N. Jr., Ziegler, W. T. 1980. *Advances in Cryogenic Engineering*, Vol. 25. New York: Plenum. 662 pp.
Buie, M. W. 1984. PhD dissertation. Univ. Ariz. 102 pp.
Buie, M. W., Cruikshank, D. P., Lebofsky, L. A., Tedesco, E. F. 1987. *Nature* 329: 522–23
Buie, M. W., Fink, U. 1987. *Icarus* 70: 483–98
Buie, M., Tholen, D. J. 1989. *Icarus* 79: 23–37
Burns, J. A. 1986. In *Satellites*, ed. J. A. Burns, M. W. Mathews, pp. 1–39. Tucson: Univ. Ariz. Press
Christy, J. W., Harrington, R. S. 1978. *Astron. J.* 83: 1005–8
Christy, J. W., Harrington, R. S. 1980. *Icarus* 44: 38–40
Clarke, J. C., Stern, S. A., Trafton, L. M. 1992. *Icarus* 95. In press
Cohen, C. J., Hubbard, E. C. 1965. *Astron. J.* 70: 10–13

Cruikshank, D. P. 1990. *Adv. Space Res.* 10(1): 199–207
Cruikshank, D. P., Pilcher, C. B., Morrison, D. 1976. *Science* 194: 835–37
Cruikshank, D. P., Silvaggio, P. M. 1979. *Ap. J.* 233: 1016–20
Cruikshank, D. P., Silvaggio, P. M. 1980. *Icarus* 41: 96–102
Cruikshank, D. P., Brown, R. H., Clarke, R. N. 1985. In *Ices in the Solar System*, ed. J. Klinger, R. Smoluchowski, pp. 817–27. Dordrecht: Reidel
Cruikshank, D. P., Brown, R. H. 1986. In *Satellites*, ed. J. A. Burns, M. S. Matthews, pp. 836–74. Tucson: Univ. Ariz. Press
Dessler, A. J., Russel, C. T. 1978. *Eos Trans. Am. Geophys. Union* 61: 690 (Abstr.)
Dobrovolskis, A. R., Harris, A. W. 1983. *Icarus* 55: 231–35
Dormand, J. R., Woolfson, M. M. 1977. *MNRAS* 180: 243–47
Dormand, J. R., Woolfson, M. M. 1980. *MNRAS* 193: 171–74
Dunbar, R. S., Tedesco, E. F. 1987. *Astron. J.* 92: 1201–10
Elliot, J. L., Dunham, E. W., Bosh, A. S., Slivan, S. M., Young, L. A., et al. 1989. *Icarus* 77: 148–70
Elliot, J. L., Young, L. A. 1991a. *Icarus* 89: 244–54
Elliot, J. L., Young, L. A. 1991b. *Astron. J.* 101: 991–1015
Eshelman, V. R. 1989. *Icarus* 80: 439–43
Farinella, P., Milani, A., Nobili, A. M., Valsecchi, G. B. 1979. *The Moon and Planets* 20: 415–21
Farinella, P., Milani, A., Nobili, A. M., Valsecchi, G. B. 1980. *Icarus* 44: 810–12
Fink, U., Smith, B. A., Benner, D. C., Johnson, R., Reitsema, H. J., et al. 1980. *Icarus* 44: 62–71
Fink, U., DiSanti, M. 1988. *Astron. J.* 95: 229–36
Fix, J. D., Neff, J. S., Kelsey, L. A. 1970. *Astron. J.* 75: 895–96
Goguen, J. D., Hammel, H. B., Brown, R. H. 1989. *Icarus* 77: 239–47
Golitsyn, G. S. 1975. *Sov. Astron. Lett.* 1: 19–20
Halliday, I., Hardie, R. H., Franz, O. G., Priser, J. B. 1966. *Publ. Astron. Soc. Pac.* 78: 113–16
Hardie, R. 1965. *Astron. J.* 70: 140
Harrington, R. S., Christy, J. W. 1980. *Astron. J.* 85: 168–70
Harrington, R. S., Christy, J. W. 1981. *Astron. J.* 86: 442–43
Harrington, R. S., Van Flandern, T. C. 1979. *Icarus* 39: 131–36
Hart, M. H. 1974. *Icarus* 21: 242–47
Hartmann, W. K., Davis, D. R. 1975. *Icarus* 24: 504–15
Hartmann, W. K., Phillips, R. J., Taylor, G. J., eds. 1986. *The Origin of the Moon.* Houston: Lunar & Planetary Inst. 1184 pp.
Hegè, E. K., Hubbard, E. N., Drummond, J. D., Strittmatter, P. A., Worden, S. P., et al. 1982. *Icarus* 50: 72–81
Hegè, E. K., Drummond, J. D. 1984. *IAU Circ. No.* 3986
Hoyt, W. G. 1980. *Planets X and Pluto.* Tucson: Univ. Ariz. Press. 136 pp.
Hubbard, W. B., Hunten, D. M., Dieters, S. W., Hill, K. M., Watson, R. D. 1988. *Nature* 336: 452–54
Hubbard, W. B., Yelle, R. V., Lunine, J. I. 1989. *Icarus* 84: 1–14
Hunten, D. M., Watson, A. J. 1982. *Icarus* 51: 665–67
Hunten, D. M., Hubbard, W. B., Dieters, S. W., Hill, K. M., Watson, R. D. 1988. *Bull. Am. Astron. Soc.* 20: 805 (Abstr.)
Johnson, R. E. 1989. *Geophys. Res. Lett.* 16: 1233–36
Jones, J. H., Christian, C. A., Waddell, P. 1988. *Publ. Astron. Soc. Pac.* 100: 489–95
Kelsey, L. A., Fix, J. D. 1973. *Ap. J.* 184: 633–36
Knacke, R. F., Geballe, T. R., Noll, K. S., Tokunaga, A. T. 1985. *Ap. J. Lett.* 298: 755–60
Kuiper, G. P. 1957. *Ap. J.* 125: 287–89
Lacis, A. A., Fix, J. D. 1972. *Ap. J.* 174: 449–53
Lebofsky, L. A., Rieke, G. H., Lebofsky, M. J. 1979. *Icarus* 37: 554–58
Lewis, J. S., Prinn, R. G. 1980. *Ap. J.* 238: 357–64
Lin, D. N. C. 1981. *MNRAS* 197: 1081–85
Lupo, M. J., Lewis, J. S. 1980a. *Icarus* 42: 29–34
Lupo, M. J., Lewis, J. S. 1980b. *Icarus* 44: 41–42
Lyttelton, R. A. 1936. *MNRAS* 97: 108–15
Marcialis, R. L. 1983. Master's thesis. Vanderbilt Univ., Nashville. 167 pp.
Marcialis, R. L. 1988. *Astron. J.* 95: 941–47
Marcialis, R. L., Lebofsky, L. A. 1991. *Icarus* 89: 255–63
Marcialis, R. L., Rieke, G. H., Lebofsky, L. A. 1987. *Science* 237: 1349–51
McKinnon, W. B. 1984. *Nature* 311: 355–58
McKinnon, W. B. 1989a. *Ap. J. Lett.* 344: L41–44
McKinnon, W. B. 1989b. *Geophys. Res. Lett.* 16: 1237–40
McKinnon, W. B., Mueller, S. 1988. *Nature* 335: 240–42
McNutt, R. L. 1989. *Geophys. Res. Lett.* 16: 1225–28
Mignard, F. 1981. *Astron. Astrophys.* 96: L1–2
Milani, A., Nobili, A. M., Carpino, M. 1989. *Icarus* 82: 200–17
Millis, R. L., Wasserman, L., Franz, O. G.,

Nye, R. A., Gilmore, A. C., et al. 1988. *Bull. Am. Astron. Soc.* 20: 806
Millis, R. L., Wasserman, L. H., Franz, O. G., Dahn, C. C., Klemola, A. R. 1989. *Eos Trans. Am. Geophys. Union* 70: 381–82 (Abstr.)
Mink, S. J., Klemola, A. R. 1985. *Astron. J.* 90: 1894–99
Mink, S. J., Klemola, A. R., Buie, M. W. 1991. *Astron. J.* 101: 2255–61
Morrison, D. 1973. *Icarus* 19: 1–14
Nacozy, P. E., Diehl, R. E. 1978. *Celest. Mech.* 17: 405–21
Neff, J. S., Lane, A. W., Fix, J. D. 1974. *Publ. Astron. Soc. Pac.* 86: 225–30
Peale, S. J. 1986. In *Satellites*, ed. J. A. Burns, M. S. Matthews, pp. 159–223. Tucson: Univ. Ariz. Press
Prinn, R. G., Fegley, B. Jr. 1981. *Ap. J.* 249: 308–17
Reinsch, K., Pakull, M. W. 1987. *Astron. Astrophys.* 177: L43–46
Reitsema, H. J., Vilas, F., Smith, B. A. 1983. *Icarus* 56: 75–79
Russell, H. N. 1906. *Ap. J.* 24: 1–18
Safronov, V. S. 1969. *NASA TTF-667*, 1972
Sawyer, S. R. 1984. Master's thesis. Univ. Texas, Austin. 204 pp.
Sawyer, S. R., Barker, E. S., Cochran, W. D., Cochran, A. L. 1987. *Science* 238: 1560–63
Seidelmann, P. K., Kaplan, G. H., Pulkkiner, K. F., Santoro, E. J., Van Flandern, T. C. 1980. *Icarus* 44: 19–28
Simonelli, D. P., Pollack, J. B., McKay, C. P., Reynolds, R. T., Summers, A. L. 1989. *Icarus* 82: 1–35
Simonelli, D. P., Reynolds, R. T. 1989. *Geophys. Res. Lett.* 16: 1209–12
Smith, B. A., Soderblom, L. A., Banfield, D., Barnett, H. C., Basilevsky, A. T., et al. 1989. *Science* 246: 1422–49
Soifer, B. T., Neugebauer, G., Matthews, K. 1980. *Ap. J.* 85: 166–67
Spencer, J. R., Buie, M. W., Bjoraker, G. L. 1990. *Icarus* 88: 491–96
Stansberry, J. A., Lunine, J. I., Tomasko, M. G. 1989. *Geophys. Res. Lett.* 16: 1221–24
Stern, S. A. 1981. Master's thesis. Univ. Texas, Austin. 170 pp.
Stern, S. A. 1988. *Icarus* 74: 269–78
Stern, S. A. 1989. *Icarus* 81: 14–23
Stern, S. A. 1991. *Icarus* 90: 271–81
Stern, S. A., Trafton, L. M. 1984. *Icarus* 57: 231–40
Stern, S. A., Trafton, L. M., Gladstone, G. R. 1988. *Icarus* 75: 485–98
Stern, S. A., Brosch, N., Barker, E. S., Gladstone, G. R. 1991a. *Icarus* 92: 332–41
Stern, S. A., Fesen, R. A., Barker, E. S., Parker, J. W., Trafton, L. M. 1991b. *Icarus* 94: 110–13
Sussman, G. J., Wisdom, J. 1988. *Science* 241: 433–37
Sykes, M. V., Cutri, R. M., Lebofsky, L. A., Binzel, R. P. 1987. *Science* 237: 1336–39
Tedesco, E. F., Veeder, G. S., Dunbar, R. S., Lebofsky, L. A. 1987. *Nature* 327: 127–29
Tholen, D. J. 1985. *Astron. J.* 90: 2353–59
Tholen, D. J., Buie, M. W., Binzel, R. P., Frueh, M. L. 1987. *Science* 237: 512–14
Tholen, D. J., Buie, M. W. 1988. *Astron. J.* 96: 1977–82
Tholen, D. J., Buie, M. W. 1989. *Bull. Am. Astron. Soc.* 21: 981 (Abstr.)
Tholen, D. J., Buie, M. W. 1990. *Bull. Am. Astron. Soc.* 22: 1129 (Abstr.)
Thompson, W. R., Murray, B. G. J. P. T., Khare, B. N., Sagan, C. 1987. *J. Geophys. Res.* 92: 14,933–41
Tombaugh, C. W., Moore, P. 1980. *Out of the Darkness: The Planet Pluto*. Harrisburg: Stackpole. 218 pp.
Trafton, L. M. 1980. *Icarus* 44: 53–61
Trafton, L. M. 1984. *Icarus* 58: 312–24
Trafton, L. M. 1990. *Ap. J.* 399: 512–23
Trafton, L. M., Stern, S. A. 1983. *Ap. J.* 267: 872–81
Trafton, L. M., Whipple, A. L., Stern, S. A. 1987. *Bull. Am. Astron. Soc.* 19: 1071–72 (Abstr.)
Trafton, L. M., Stern, S. A., Gladstone, G. R. 1988b. *Icarus* 74: 108–20
Tyler, G. E., Sweetman, D. M., Anderson, J. D., Borutzki, S. E., Campbell, J. K., et al. 1989. *Science* 246: 1466–73
Wagner, J. K., Hapke, B. W., Wells, E. 1987. *Icarus* 69: 14–37
Walker, A. R. 1980. *MNRAS* 192: 47P–50P
Walker, M. F., Hardie, R. 1955. *Publ. Astron. Soc. Pac.* 67: 224–31
Wasserman, L. H., Millis, R. L., Franz, O. G., Klemola, A. R., Dahn, C. C. 1988. *Bull. Am. Astron. Soc.* 20: 806 (Abstr.)
Watson, A. J., Donahue, T. M., Walker, J. C. G. 1981. *Icarus* 48: 150–66
Weissman, P. R., Dobrovolskis, A. R., Stern, S. A. 1989. *Geophys. Res. Lett.* 16: 1241–44
Whipple, A. L., Trafton, L. M., Stern, S. A. 1989. *Bull. Am. Astron. Soc.* 21: 982 (Abstr.)
Whyte, A. J. 1980. *The Planet Pluto*. Toronto: Pergamon. 147 pp.
Williams, J. G., Benson, G. S. 1971. *Astron. J.* 76: 167–71
Yelle, R. V., Lunine, J. I. 1989. *Nature* 339: 288–90